




Combinations of Toll-like receptor 8 agonist TL8-506 activate human tumor-derived dendritic cells

Mi He ¹, Bhavesh Soni,² Petra C Schwalie,² Tamara Hüsser,¹ Caroline Waltzinger,¹ Duvini De Silva,¹ Ylva Prinz,¹ Laura Krümpelmann,³ Samuele Calabro,¹ Ines Matos,¹ Christine Trumfheller,¹ Marina Bacac,¹ Pablo Umaña,¹ Mitchell P Levesque,⁴ Reinhard Dummer ⁴, Maries van den Broek ⁵, Stephan Gasser¹

To cite: He M, Soni B, Schwalie PC, *et al.* Combinations of Toll-like receptor 8 agonist TL8-506 activate human tumor-derived dendritic cells. *Journal for ImmunoTherapy of Cancer* 2022;**10**:e004268. doi:10.1136/jitc-2021-004268

► Additional supplemental material is published online only. To view, please visit the journal online (<http://dx.doi.org/10.1136/jitc-2021-004268>).

Accepted 27 April 2022



© Author(s) (or their employer(s)) 2022. Re-use permitted under CC BY-NC. No commercial re-use. See rights and permissions. Published by BMJ.

For numbered affiliations see end of article.

Correspondence to
Mi He; mi.he@roche.com

Dr Stephan Gasser;
stephan.gasser@roche.com

ABSTRACT

Background Dendritic cells (DCs) are professional antigen presenting cells that initiate immune defense to pathogens and tumor cells. Human tumors contain only few DCs that mostly display a non-activated phenotype. Hence, activation of tumor-associated DCs may improve efficacy of cancer immunotherapies. Toll-like receptor (TLR) agonists and interferons are known to promote DC maturation. However, it is unclear if DCs in human tumors respond to activation signals and which stimuli induce the optimal activation of human tumor DCs.

Methods We first screened combinations of TLR agonists, a STING agonist and interferons (IFNs) for their ability to activate human conventional DCs (cDCs). Two combinations: TL8-506 (a TLR8 agonist)+IFN- γ and TL8-506+Poly(I:C) (a TLR3 agonist) were studied in more detail. cDC1s and cDC2s derived from cord blood stem cells, blood or patient tumor samples were stimulated with either TL8-506+IFN- γ or TL8-506+Poly(I:C). Different activation markers were analyzed by ELISA, flow cytometry, NanoString nCounter Technology or single-cell RNA-sequencing. T cell activation and migration assays were performed to assess functional consequences of cDC activation.

Results We show that TL8-506 synergized with IFN- γ or Poly(I:C) to induce high expression of different chemokines and cytokines including interleukin (IL)-12p70 in human cord blood and blood cDC subsets in a combination-specific manner. Importantly, both combinations induced the activation of cDC subsets in patient tumor samples *ex vivo*. The expression of immunostimulatory genes important for anticancer responses including *CD40*, *IFNB1*, *IFNL1*, *IL12A* and *IL12B* were upregulated on stimulation. Furthermore, chemokines associated with CD8⁺ T cell recruitment were induced in tumor-derived cDCs in response to TL8-506 combinations. In vitro activation and migration assays confirmed that stimulated cDCs induce T cell activation and migration.

Conclusions Our data suggest that cord blood-derived and blood-derived cDCs are a good surrogate to study treatment responses in human tumor cDCs. While most cDCs in human tumors display a non-activated phenotype, TL8-506 combinations drive human tumor cDCs towards an immunostimulatory phenotype associated with Th1 responses on stimulation. Hence, TL8-506-based

WHAT IS ALREADY KNOWN ON THIS TOPIC

⇒ In human tumors, the majority of conventional dendritic cells shows an inactivated phenotype. It is unclear if they can be converted into activated and immunostimulatory dendritic cells.

WHAT THIS STUDY ADDS

⇒ Our study shows that patient tumor-derived conventional dendritic cells from different cancer indications can be activated by Toll-like receptor 8 agonist combinations to express chemokines and proinflammatory cytokines including interleukin-12 and type I interferons.

HOW THIS STUDY MIGHT AFFECT RESEARCH, PRACTICE AND/OR POLICY

⇒ Toll-like receptor 8 agonist-based combinations may enhance antitumor immunity in patients with cancer by targeting and activating conventional dendritic cells in the tumor microenvironment.

combinations may be promising candidates to initiate or boost antitumor responses in patients with cancer.

BACKGROUND

Dendritic cells (DCs) are specialized antigen presenting cells, which are essential for the initiation and orchestration of the adaptive immunity against pathogens or tumor cells.^{1,2} DCs are crucial for priming of tumor antigen-specific T cells in the tumor draining lymph nodes.³ In addition, DCs support T cell effector functions in the tumor microenvironment.^{4,5} However, the generation of immunostimulatory DCs depends on appropriate activation cues counterbalancing potential suppressive factors in the tumor microenvironment.^{6,7} Recent single-cell RNA-sequencing (scRNA-seq) data confirmed that only a small population of DCs in human tumors expresses maturation markers such

as *CCR7* and *LAMP3*, whereas most DCs display a non-activated phenotype.^{7,8}

DCs in human tumors consist of conventional DC (cDC)1 and cDC2 subsets.^{7,8} cDC1s are present in blood and tissues in low numbers. They are identified by the expression of CLEC9A, an endocytic receptor for actin filaments exposed on dead cells that favors cross-presentation of cell-associated antigens.⁹ Therefore, cDC1s can efficiently cross-present endocytosed tumor antigens to CD8⁺ T cells.¹⁰ The more abundant and heterogeneous cDC2s express CD1c and CLEC10A, markers that are shared to some extent with other immune cell types such as monocytes or macrophages.¹¹ cDC2s are thought to mainly activate CD4⁺ helper T cells because of their high expression of major histocompatibility complex (MHC)-II pathway-associated genes and co-localization with CD4⁺ T cells in secondary lymphoid organs.^{12,13} However, some studies have challenged these strict functional separations and highlighted the importance of cDC1–cDC2 crosstalk for effective antitumor immunity.¹⁴ Human cDC2s, when properly activated, can produce high amounts of interleukin (IL)-12p70 and efficiently cross-present viral antigens to CD8⁺ T cells.¹⁵ In this context, it is interesting that the phenotypes of cDC1 and cDC2 converge on activation and display a similar gene expression profile.^{7,8}

Harnessing the potential of DCs for cancer immunotherapy has gained interest since several studies have found a correlation of DC gene signatures in human tumors with improved response to immune checkpoint inhibitors and patient survival.^{16,17} Along the same lines, it was shown in preclinical models that DC activation promoted T cell infiltration into the tumor, restricted tumor growth and prolonged survival.^{18,19}

Pattern recognition receptor (PRR) agonists and interferons (IFNs) can induce DC maturation and promote their immunostimulatory functions.^{20–22} Although a synergy between PRR agonists and IFNs concerning IL-12p70 expression and T cell activation was described,^{23,24} it is unclear which stimuli induce the optimal activation of cDCs in human tumors.

Toll-like receptor 8 (TLR8), a PRR, is expressed on both cDC subsets in humans.^{8,21} Although TLR8 agonists were tested in the past and are currently being evaluated for the treatment of different human cancer indications including head and neck or ovarian cancer in clinical trials (NCT03906526, NCT04460456, NCT02431559, NCT01836029), their effects on human tumor-derived cDC1s and cDC2s are unknown.

Here, we tested various combinations of TLR agonists, a STING agonist and IFNs for their ability to activate cDCs. TLR8 agonist TL8-506 synergized with TLR3 agonist Poly(I:C) or IFN- γ in the expression of combination-specific cytokines in human cord blood and blood cDC subsets. Importantly, TL8-506-based combinations activated both cDC1s and cDC2s derived from tumor explants of patients with cancer. To our knowledge this is the first study that shows the ex vivo activation of patient tumor-derived cDCs from different solid tumor indications and

investigates the molecular alterations in activated human tumor cDCs. Our results suggest that targeting TL8-506-based combinations to tumor cDCs may open new opportunities to improve antitumor immunity in patients with cancer.

MATERIALS AND METHODS

Human samples

Human cord blood CD34⁺ stem cells were purchased from STEMCELL Technologies (#70008). Buffy coats were obtained from the Blood Donation Center Zurich (BASEC-Nr: 2020–01208). Frozen dissociated lung and ovarian tumor cells were purchased from Discovery Life Sciences, Huntsville, Alabama, USA. Melanoma and colorectal tumor samples were obtained from University Hospital of Zurich (BASEC-Nr.2017–00494) and Hirslanden Klinik Zurich (BASEC-Nr: 2016–02013). Declaration of informed consent was signed by all patients for all samples.

Isolation of peripheral blood mononuclear cells

Peripheral blood mononuclear cells (PBMCs) were isolated from buffy coats using the SepMate PBMC Isolation Tubes (STEMCELL Technologies, #85450) according to the manufacturer's instructions.

Enrichment of DCs from blood

DCs were enriched from freshly isolated PBMCs using the Miltenyi PanDC Enrichment Kit (#130-100-777) according to the manufacturer's protocol and 2 \times enrichment was performed for all experiments.

Expansion of cord blood stem cells

1 \times 10⁶ CD34⁺ cord blood stem cells were thawed in a 37°C water bath and pipetted into 20 mL pre-warmed StemSpan SFEM medium (STEMCELL Technologies, #09650). Cells were centrifuged and resuspended into StemSpan medium containing 10% fetal bovine serum (FBS) (Sigma, #F4135). Cells were adjusted to 2.5 \times 10⁴ cells/mL, supplemented with 20 ng/mL huIL-3 (Pepro-Tech, #200–03), 100 ng/mL huSCF (PeproTech, #300–07), 100 ng/mL huFLT3L (PeproTech, #300–19), 50 ng/mL huTPO (PeproTech, #300–18), plated at 0.5 \times 10⁴ cells per well in a 96-well U bottom plate and cultured at 37°C in a CO₂ incubator. After 7 days of expansion, cells were harvested and frozen in 80% MEM- α (Gibco, #12 561–056), 10% DMSO (Sigma, #D2650), 10% FBS at 2.6 \times 10⁶ cells/mL. Cells were stored in liquid nitrogen.

Differentiation of DCs from cord blood stem cells

Murine stromal MS-5 cells were obtained from DMCZ (#ACC 441) and cultured in MS-5 medium (MEM- α , Gibco, #15 070–063, 10% FBS, 1% Pen/Strep, Gibco, #15 070–063, 2 mM Sodium Pyruvate, Gibco, #11 360–039). For in vitro cord blood DC differentiation, MS-5 cells were treated with 10 μ g/mL Mitomycin C (Sigma, #M4287) for 3 hours at 37°C to stop cell proliferation. After washing, cells were detached by Trypsin-EDTA

(Gibco, #25 300–054) and plated at 2.5×10^5 cells/mL in 100 μ L volume per well in a 96-well F bottom plate. The day after, expanded CD34⁺ cord blood stem cells were added to the pre-treated MS-5 cells to start DC differentiation. 2.6×10^6 frozen cord blood stem cells were thawed and washed once. Cells were resuspended in 20 mL MS-5 medium supplemented with 5 ng/mL huGM-CSF (PeproTech, #300–03), 5 ng/mL huIL-4 (PeproTech, #200–04), 40 ng/mL huSCF and 200 ng/mL huFLT3L. 100 μ L cord blood stem cells at 1.3×10^5 cells/mL were added to each well to the plated MS-5 cells in the 96-well F bottom plates and cultured at 37°C in a CO₂ incubator. Cells were fed on day 6 with 50 μ L/well MS-5 medium supplemented with 12.5 ng/mL huGM-CSF, 12.5 ng/mL huIL-4, 100 ng/mL huSCF and 500 ng/mL huFLT3L. In vitro differentiated cord blood DCs were harvested on day 12 or 13 after initiation of the culture.

Digestion of tumor tissue

Human tumor tissues were cut with a scalpel into small pieces at room temperature in the presence of 0.5 mL digestion mix (50% Accutase, Sigma, #A6964, 44% MACS Tissue Storage Solution, Miltenyi, #130-100-008, 1% BSA, Sigma, #A9576, 275 U/mL Collagenase IV, Worthington, LS004189, 10 U/mL DNase I Type 4, Sigma, #D5025, 471 U/mL Hyaluronidase, Sigma, #H6254). Pieces were further incubated with 10 mL digestion mix for 20–30 min at 37°C on a Miltenyi MACS rotator with medium speed. Cells were harvested through a 70 μ m cell strainer on ice and remaining tumor pieces were carefully mashed through the cell strainer with the plunger of a 10 mL syringe. The tumor digestion solution was then centrifuged for 15 min at $300 \times g$, 4°C and the supernatant was carefully removed. Dissociated tumor cells were resuspended in cold RPMI medium (Gibco, #42 401–042) and counted. Cells were stored at $1\text{--}5 \times 10^6$ cells/mL in freezing medium (IBIDI, #89020) in liquid nitrogen.

Stimulation of DCs

Enriched blood DCs or sorted cord blood cDCs were resuspended at 1×10^6 cells/mL, PBMCs or tumor digests were resuspended at $5\text{--}10 \times 10^6$ cells/mL in DC medium (RPMI GlutaMAX, Gibco, #72 400–021, 1% human serum, Sigma, #H4522, 1% Pen/Strep). 1×10^5 cells (enriched blood DCs or sorted cord blood cDCs) or $0.5\text{--}1 \times 10^6$ cells (PBMCs or tumor digests) in 200 μ L/well were treated with the indicated stimuli in a 96-well plate at 37°C in a CO₂ incubator. For DC activation in the presence of tumor-conditioned medium, 1:1 diluted supernatant from a 6-hour culture of patient-derived tumor digest in DC medium or a 2-day culture of COR-L105 tumor cell line (ECACC, #92031918) in RPMI GlutaMAX, 10% FBS, 1% Pen/Strep was added to sorted cord blood cDCs during stimulation. The following concentrations were used: 10'000 U/mL huIFN- α (R&D, #11100–1), 10'000 U/mL huIFN- β (R&D, #8499-IF-010), 1 μ g/mL huIFN- λ (R&D, #1598-IL-025), 50'000 U/mL huIFN- γ (PeproTech, #300–02), 1 μ g/mL Pam3CSK4 (Invivogen, #vac-pms), 10

μ g/mL Poly(I:C) (Invivogen, #vac-pic), 0.1 μ g/mL LPS (Sigma, #L2880), 1 μ M TL8-506 (Invivogen, #tlrl-tl8506), 10 μ M CL075 (Invivogen, #tlrl-c75), 10 μ M R848 (Invivogen, #vac-r848), 10 μ g/mL ssRNA40 (Invivogen, #tlrl-lrna40), 10 μ g/mL 2'3'-cGAM(PS)2(Rp/Sp) (Invivogen, #tlrl-nacga2srs).

Quantification of cytokines and chemokines in DC supernatant

1×10^5 enriched blood DCs or sorted cord blood cDCs were stimulated in 200 μ L DC medium/well in a 96-well U bottom plate at 37°C in a CO₂ incubator for 18 hours. Stimulated cells were centrifuged at $300 \times g$ for 5 min. DC supernatants were collected and cytokine concentrations were determined using either Cisbio human cytokine HTRF kits (Cisbio, #62HIL12PEG) or customized ProcartaPlex Multiplex kits (Life Technologies).

Flow cytometry

$0.5\text{--}1 \times 10^6$ PBMCs or tumor digests were stimulated in 200 μ L DC medium/well in a 96-well V bottom plate at 37°C in a CO₂ incubator for 3 hours in total, with GolgiPlug 1:1000 (BD, #555029) added after 1 hour stimulation. Stimulated cells were centrifuged at $300 \times g$ for 5 min at room temperature. Cells were resuspended in 50 μ L/well human BD Fc block 1:50 in eBioscience staining buffer (eBioscience, #0-4222-26) and incubated for 15 min at 4°C. After removal of human BD Fc block, cells were incubated with the indicated antibodies in Brilliant Stain Buffer (BD, #566349) for 20 min at 4°C. For intracellular staining, cells were washed, fixed and permeabilized using the Foxp3 staining buffer set (eBioscience, #00-5523-00). Antibodies for intracellular staining were incubated with cells for 20 min at 4°C. Cells were washed, resuspended in eBioscience staining buffer and acquired on the BD LSRFortessa or BD FACSymphony A5. Data were analyzed using FlowJo V.10. cDC1s were gated as CD45⁺, CD3⁻, CD56⁻, CD16⁻, CD14⁻, CD19⁻, CD68⁻, MHC-II⁺, CD11c⁺ and CLEC9A⁺ cells. cDC2s were gated as CD45⁺, CD3⁻, CD56⁻, CD16⁻, CD14⁻, CD19⁻, CD68⁻, MHC-II⁺, CD11c⁺ and CD1c⁺ cells. CXCL9, CXCL10, IFN- λ , TNF- α , CLEC9A and CD68 were stained intracellularly. Further details of the used antibodies are listed in online supplemental table 1.

Fluorescence-activated cell sorting of cord blood DCs

In vitro differentiated cord blood DCs were harvested on day 12 or 13 and filtered through a 40 μ m cell strainer. Cells were centrifuged at $300 \times g$ for 5 min and resuspended at 10×10^6 cells/mL in ice cold phosphate-buffered saline (PBS) containing 1:50 human BD Fc block (BD, #564220). Cells were incubated for 15 min on ice. Cells were centrifuged at $300 \times g$ for 5 min, human BD Fc block was removed and cells were stained with antibodies in PBS for 20 min on ice. Cells were washed with ice cold PBS, passed through a 35 μ m cell strainer and resuspended at 10×10^6 cells/mL in ice cold PBS for sorting on a BD FACSAria III. cDC1s were sorted as CD45⁺, CD14⁻, CLEC9A⁺ and CD141⁺ cells. cDC2s were sorted as CD45⁺,

CD14⁻, CLEC9A⁻, CD141⁻ and CD1c⁺ cells. Sorting speed was kept below 4000 events/s.

NanoString nCounter gene expression analysis

1×10⁵ sorted cord blood cDCs were stimulated in 200 µL DC medium/well in a 96-well U bottom plate for 15 hours at 37°C in a CO₂ incubator. Cells were collected, centrifuged at 300 × g for 5 min and washed 1× with PBS. 1×10⁵ cells were lysed in 5 µL RLT buffer containing 0.142 M β-mercaptoethanol (Qiagen, #79216, Bio-Rad, #1610710) on ice and vortexed for 1 min. Cell lysates were snap frozen and stored at -80°C. 1.5 µL cell lysate was used for each NanoString reaction. Messenger RNA expression was detected using the human Myeloid Innate Immunity panel (NanoString, #115000171) according to the manufacturer's instructions. In brief, samples were hybridized to the CodeSet probes for 24 hours at 65°C. Samples were then processed on NanoString nCounter and gene counts were normalized to the 40 reference genes provided by the panel.

Single-cell RNA-sequencing

Patient tumor digests were stimulated at 1×10⁶ cells/well in 200 µL DC medium/well in a 96-well V bottom plate for 4 hours at 37°C in a CO₂ incubator. Cells were harvested and incubated with 1:25 human BD Fc block for 10 min on ice. Human BD Fc block was removed and cells were stained with antibodies in PBS for 20 min on ice. Cells were washed, passed through a 35 µm cell strainer and resuspended in ice cold PBS for sorting. Live CD45⁺, CD3⁻ single cells were sorted for scRNA-seq. 1×10⁴ sorted cells per condition were loaded on the 10x Genomics Chromium Connect. The automated single cell library construction workflow was applied using Single Cell 3' kit V.3.1 (#PN-1000128, #PN-1000127, #PN-1000213) purchased from 10x Genomics. Pooled libraries were sequenced at the Functional Genomics Center Zurich on the Illumina NextSeq 2000.

ScRNA-seq data analyses

Publicly available scRNA-seq data sets of different tissues (online supplemental table 2) were collected either as raw count matrices or fastq files. Internal and external fastq files were aligned and quantified using the Cell Ranger Single-Cell Software²⁵ with default parameters against the GRCh38 human reference genome. The data were further pre-processed by following the standard workflow in Besca.²⁶ For each data set, the genes showing highest variability using `besca.st.highly_variable_genes` function were selected. Principal component analysis with 50 components was performed and the first 50 components retained to build a nearest neighbor graph and to derive clusters using the Leiden community detection algorithm.²⁷ To identify the cell type of the clusters returned by the Leiden algorithm, curated signatures and the `sig-annot` workflow available in Besca were used based on the expression of signature markers, applying the filter parameters in online supplemental

table 3.²⁶ Differential expression (DE) analysis between different cell groups was performed using a Wilcoxon rank-sum test and multiple hypothesis testing correction using the Benjamini-Hochberg procedure (`function scanpy.tl.rank_genes_groups`). Top 50 DE genes based on the highest log₂FC change and adjusted p-value less than 0.05 are listed in online supplemental table 4. The Velocity V.0.17.17 package²⁸ was used to obtain spliced and unspliced read counts from the previously aligned scRNA-seq files from melanoma, lung and colon cancer samples and RNA velocity was calculated using the `scvelo V.0.2.3` package.²⁹ The detailed procedure for scRNA-seq data analyses is described in Supplementary Materials.

HEK-Blue reporter cell assay

HEK-Blue huTLR7 (Invivogen, #hkb-htlr7) and HEK-Blue huTLR8 (Invivogen, #hkb-htlr8) were maintained according to manufacturer's recommendations. 4×10⁴ HEK-Blue cells were treated with the indicated stimuli in 200 µL HEK-Blue Detection medium/well in a 96-well F bottom plate for 18 hours at 37°C in a CO₂ incubator. Secreted embryonic alkaline phosphatase (SEAP) expression was measured using HEK-Blue Detection (Invivogen, #hb-det2) according to manufacturer's instructions.

Activation of naive T cells by DCs

1×10⁵ sorted cord blood cDCs were stimulated in 200 µL DC medium/well in a 96-well U bottom plate for 18 hours at 37°C in a CO₂ incubator. Stimulated cDCs were then washed three times with DC medium to remove remaining stimuli. Naive T cells were isolated from PBMCs using the Miltenyi Naive Pan T Cell Isolation Kit (#130-097-095) according to the manufacturer's protocol. 1×10⁵ isolated naive T cells were co-cultured 5:1 with 2×10⁴ stimulated cDCs for 4 days at 37°C in a CO₂ incubator. Cytokine in cell culture supernatants was quantified using the Cisbio human IFN-γ HTRF kit (#62HIFNGPET) or customized ProcartaPlex Multiplex kits (Life Technologies).

DC migration assay

1×10⁵ sorted cord blood cDCs were stimulated in 200 µL/well OPTI-MEM (Gibco, #31985062) in a 96-well U bottom plate for 18 hours at 37°C in a CO₂ incubator and supernatant was collected. 100 µL of supernatant were diluted 1:1 with OPTI-MEM and plated in the lower compartment of a transwell plate. Transwell inlets with 5 µm pore size (Corning, #CLS3387-8EA) were used and 5×10⁵ cells of cord blood DC culture at day 13 were added in 100 µL volume to the inlets. DCs were allowed to migrate for 3 hours and the sum of cord blood cDC1s and cDC2s migrated to the lower compartment was quantified by flow cytometry. Normalization for absolute counting of cells was performed using 123count eBeads (Invitrogen, #01-1234-42) according to the manufacturer's instructions.

CD8⁺ T cell migration assay

T cell migration assays were performed in three-lane OrganoPlate (MIMETAS, #4004-400-B) using collagen

as extracellular matrix barrier and human umbilical vein endothelial cells (HUVECs) (Lonza, #C2517AS) for vessel formation. Isolated CD8⁺ T cells (Miltenyi, #130-096-495) were activated by CD3/CD28 cross-linking (STEMCELL, #10971) and labeled with CFDA (Life Technologies, #C7025). T cell migration towards supernatants of stimulated cord blood cDCs or recombinant cytokine dilutions was measured after 48 hours using the PerkinElmer Operetta High Content Imaging System. Quantification of the migrated T cells was done using ImageJ. The detailed experimental procedure is described in Supplementary Materials.

Statistics

For comparison of two groups, Student's t-test was used. For comparison of multiple groups one-way analysis of variance was performed with Tukey's multiple comparison correction. Statistical tests were performed using GraphPad Prism V.8. Error bars show SD if not otherwise specified.

Illustrations

The graphical abstract and illustrations were created with BioRender.com.

RESULTS

TL8-506-based combinations synergize to induce the production of proinflammatory cytokines and chemokines by human cord blood DCs

To identify stimuli for tumor DC activation, we screened combinations of TLR agonists, a STING agonist and IFNs, which could induce strong secretion of IL-12p70, an important mediator of DC functions for Th1 T cell responses.³⁰ IL-12p70 supports the expansion of naive T cells during T cell priming and promotes IFN- γ release in T cells.^{31,32} Different TLR agonists, a STING agonist and IFNs were tested as single stimuli and in combinations in enriched human blood DC cultures. TL8-506, a TLR8-selective agonist, synergized with other stimuli to induce the highest concentrations of IL-12p70 in the supernatant among the tested combinations (figure 1A, online supplemental figure S1). Strong IL-12p70 secretion was observed for TL8-506+Poly(I:C) and this synergistic effect was not restricted to TL8-506, but detected for different TLR8 agonists in combination with Poly(I:C) (figure 1B).

To study the effects of the combinations in specific cDC subsets and exclude the possibility that IL-12p70 was produced by other cells in the enriched blood DC fractions, we sorted cord blood stem cell-derived cDCs before stimulation with the different TL8-506 combinations. cDCs differentiated in vitro from cord blood stem cells can be generated in higher numbers and transcript expression analysis showed comparable overall gene expression to blood and tumor cDCs (online supplemental figure S2A,B). This assessment was based on an integrated collection of reanalyzed publicly available data that resulted in a reference map of cDCs across tissues and

cancer indications (online supplemental table 2).^{7,8,33-43}

We performed scRNA-seq of in vitro differentiated cord blood cDCs and blood cDCs, and compared their gene expression with those present in healthy tissues and different tumor indications of public scRNA-seq studies. Both cord blood cDC subsets expressed the cDC subset-specific markers, PRRs and IFNRs (online supplemental figure S2C,D), suggesting their relevance for our screening experiments. In accordance with the findings in enriched blood DC cultures, TL8-506 combinations induced the highest amount of IL-12p70 in supernatants of cord blood cDCs among the tested treatments (figure 1C). Synergy in IL-12p70 induction by IFN- γ +TL8-506 and Poly(I:C)+TL8-506 stimulation was consistently detected in all tested donors and experiments (figure 1D). We selected these two TL8-506 combinations to study in more detail, as IFN- γ , TLR3 agonists and TLR8 agonists are potentially clinically relevant molecules, which are currently being evaluated in clinical trials for cancer treatment (NCT02614456, NCT02834052, NCT01976585, NCT03732547).

Next, we analyzed the expression of chemokines and cytokines other than IL-12p70. As a single stimulus, each compound induced a specific cytokine profile and combinations selectively synergized in the expression of certain cytokines (figure 1E). TL8-506 in combination with Poly(I:C) induced the highest release of IL-12 family cytokines (IL-12p70, IL-23, IL-27), IFNs (IFN- β , IFN- λ), different proinflammatory cytokines (tumor necrosis factor (TNF)- α , IL-6, IL-1 α , IL-1 β) and chemokines (CCL3, CCL4, CCL20). IFN- γ +TL8-506 synergized in the induction of IFN- γ -inducible chemokines (CXCL9, CXCL10, CXCL11). Gene expression data further supported these combination-specific synergies (online supplemental figure S3A,B). For most cytokines including IL-12p70, secretion was stronger in cDC2s compared with cDC1s in response to treatment with TL8-506 combinations (figure 1E).

TL8-506-based combinations synergize to activate human blood DC subsets

We next tested the effects of TL8-506-based combinations in cDC subsets derived from peripheral blood, a more physiologically relevant source of cDCs. As the numbers of blood cDCs were limiting, we focused on a selection of cytokines and chemokines that were synergistically induced by TL8-506-based combinations (figure 1E). Consistent with observations in cord blood cDCs, CXCL9 and CXCL10 expression was induced by IFN- γ and the percentage of CXCL9 or CXCL10 positive cDCs was further increased by the combination with TL8-506. Similarly, IFN- λ was induced by Poly(I:C) in cDC1s and its expression was further amplified by combination with TL8-506. TNF- α was induced by TL8-506 and combination with Poly(I:C) further enhanced this effect (figure 2A). Co-production of TNF- α and CXCL10 was only induced by combinatorial IFN- γ +TL8-506 stimulation (figure 2B,C) whereas the co-expression of TNF- α and IFN- λ was only

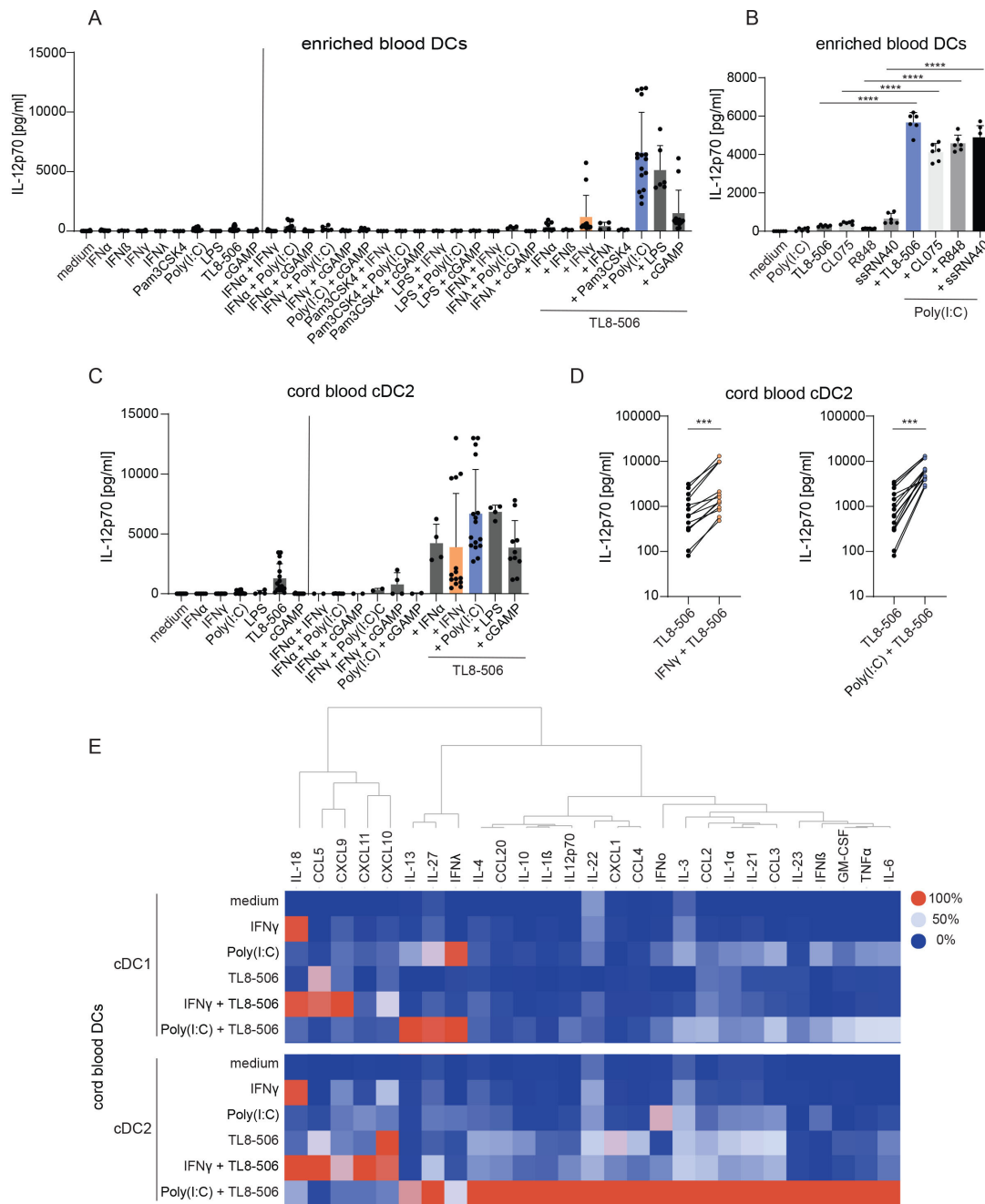


Figure 1 TL8-506-based combinations synergize in cytokine and chemokine secretion in cord blood DC subsets. (A, B) Enriched blood DCs were stimulated for 18 hours with the indicated stimuli. IL-12p70 concentrations were measured in the cell culture supernatant by ELISA. (A) IL-12p70 concentrations in enriched blood DC cultures on stimulation with combination of agonists, $n = \text{two} - \text{eight}$ donors, from one to six independent experiments, mean+SD is shown. (B) IL-12p70 concentrations in enriched blood DC cultures on stimulation with combination of Poly(I:C) and different TLR8 agonists, $n = 4$ donors, two independent experiments, representative data of two donors from one experiment, mean+SD is shown. One-way analysis of variance was used for statistical analysis, $****p \leq 0.0001$. (C – E) Sorted cord blood DCs were stimulated for 18 hours with the indicated stimuli. Cytokine concentrations were determined in the cell culture supernatant by ELISA. (C) IL-12p70 concentrations in the supernatant of sorted cord blood cDC2s on stimulation with combination of agonists, $n = \text{two} - \text{seven}$ batches of cord blood from mixed donors, from two to eight independent experiments, mean+SD is shown. (D) IL-12p70 concentrations in the supernatant of cord blood cDC2s treated with TL8-506 alone or in combination with IFN- γ or Poly(I:C), $n = \text{seven}$ batches of cord blood from mixed donors, 14 donors in total, from seven independent experiments, paired Student's t-test, $***p \leq 0.0002$. (E) Cytokine concentrations in the supernatant of cord blood cDC1s and cDC2s treated with the indicated stimuli, $n = \text{three}$ batches of cord blood from mixed donors, 6 donors in total, from three independent experiments, colors displaying the maximum (100%) to minimum (0%) mean cytokine concentrations per column. The following concentrations were used for DC stimulation: 10^4 U/mL huIFN- α , 10^4 U/mL huIFN- β , $1 \mu\text{g}/\text{mL}$ huIFN- λ , 50^4 U/mL huIFN- γ , $1 \mu\text{g}/\text{mL}$ Pam3CSK4, $10 \mu\text{g}/\text{mL}$ Poly(I:C), $0.1 \mu\text{g}/\text{mL}$ LPS, $1 \mu\text{M}$ TL8-506, $10 \mu\text{M}$ CL075, $10 \mu\text{M}$ R848, $10 \mu\text{g}/\text{mL}$ ssRNA40, $10 \mu\text{g}/\text{mL}$ 2'3'-cGAM(PS)2(Rp/Sp). cDC, conventional DC; DC, dendritic cell; IFN, interferon; IL, interleukin.

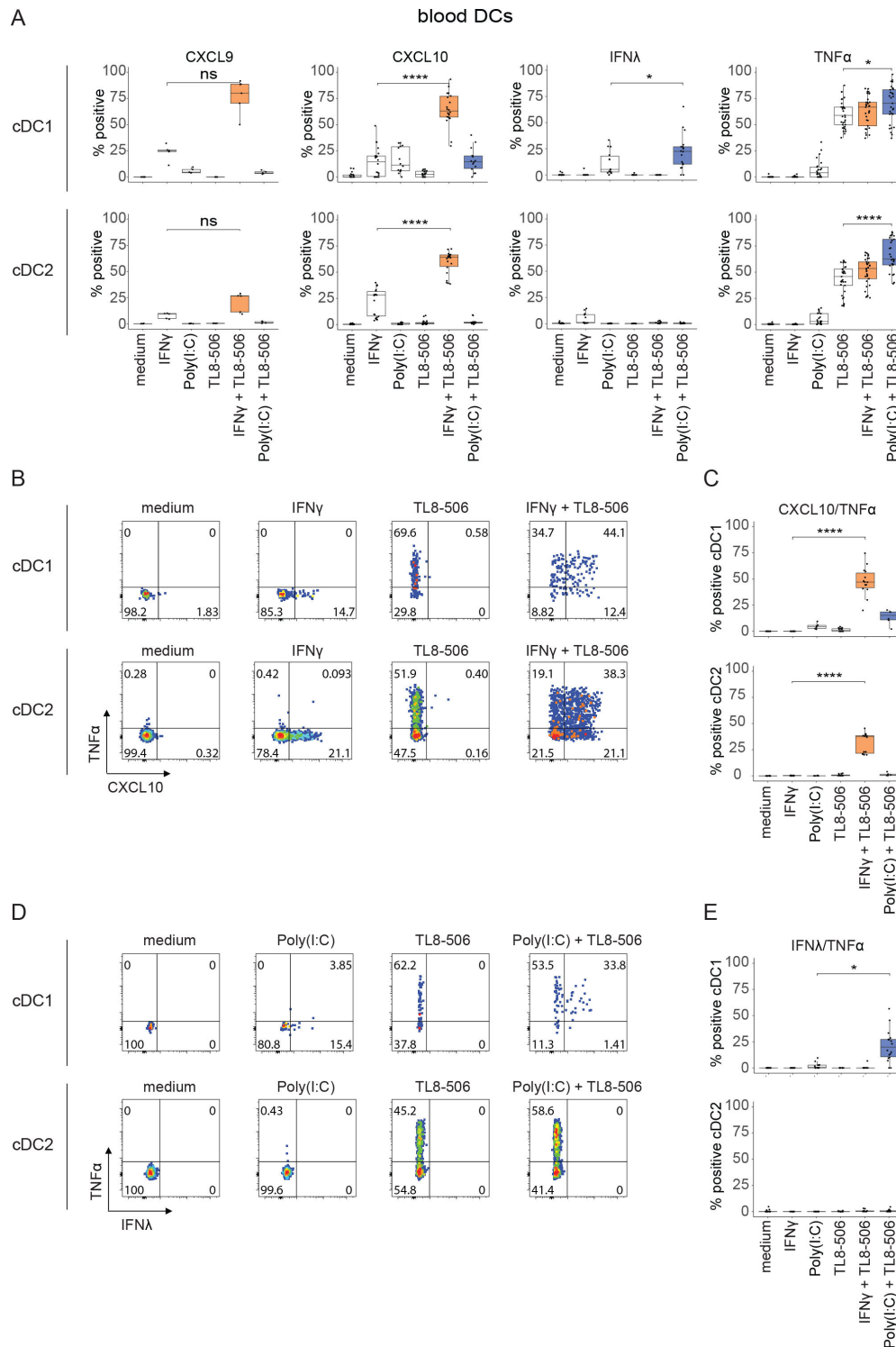


Figure 2 TL8-506-based combinations synergize in the production of cytokines and chemokines in human blood DC subsets. Human peripheral blood mononuclear cells (PBMCs) were treated with the indicated stimuli for three hours. Intracellular cytokine staining was performed and analyzed by flow cytometry. (A) Quantification of cytokine producing blood cDCs, n =two–11 donors, from two to 16 independent experiments. (B) Flow cytometry plots of IFN- γ +TL8-506 and single stimuli treated blood cDCs showing the distribution of CXCL10 or/and TNF- α expressing cDCs. Percentage of positive cells are indicated in the quadrants. (C) Quantification of CXCL10/TNF- α double positive blood cDCs on stimulation with the indicated stimuli, n =four–eight donors, from four to eight independent experiments. (D) Flow cytometry plots of Poly(I:C)+TL8-506 and single stimuli treated blood cDCs showing the distribution of IFN- λ or/and TNF- α expressing cDCs. Percentage of positive cells are indicated in the quadrants. (E) Quantification of IFN- λ /TNF- α double positive blood cDCs on stimulation with the indicated stimuli, n =four–six donors, from four to six independent experiments. Statistics for A, C, E: paired Student's t-test, * p \leq 0.03, **** p \leq 0.0001, ns, not significant. The following concentrations were used for DC stimulation: 50'000 U/mL huIFN- γ , 10 μ g/mL Poly(I:C), 1 μ M TL8-506. cDC, conventional DC; DC, dendritic cell; IFN, interferon; TNF, tumor necrosis factor.

triggered by combinatorial Poly(I:C)+TL8-506 treatment (figure 2D,E). Taken together, our data show that similar to cord blood cDCs, blood cDC1s and cDC2s are activated by TL8-506 combinations, which synergize in a stimulus-specific manner.

TL8-506 combinations activate DCs in human tumors

cDCs with an activated phenotype are scarce in different human tumor indications (online supplemental figure S4A,B), therefore we attempted to test whether the two selected TL8-506 combinations could activate cDCs in patient tumor explants *ex vivo*. To comprehensively analyze the effects of TL8-506 combinations on patient tumor-derived cDCs, we performed scRNA-seq of stimulated tumor cDCs derived from two melanoma samples of lymph node metastases, one colorectal cancer (CRC) sample of liver metastasis and one lung adenocarcinoma sample. Percentages of CD45⁺ cells in tested samples are shown in the supplementary files (online supplemental table 5). IFN- γ +TL8-506 and Poly(I:C)+TL8-506 stimulated cDCs clustered separately from untreated cDCs (figure 3A) and showed upregulation of many known DC activation markers (figure 3B). Important signals for T cell activation such as *IL12A*, *IL12B*, *IL15*, *CD40* were induced by both TL8-506 combinations. In contrast, the expression of the CD8⁺ T cell recruiting chemokines *CXCL9*, *CXCL10*, *CXCL11* and their co-expression with *TNF* was specific to the IFN- γ +TL8-506 combination (figure 3B,C). The expression of *IFNB1* and *IFNL1* was specific to the Poly(I:C)+TL8-506 combination, as previously observed for cord blood and blood-derived cDCs. Of note, both cDC1s and cDC2s showed comparable gene induction and increased *IL12A* and *IL12B* expression on stimulation with the two TL8-506 combinations. Differential expression (DE) analysis confirmed that *CXCL9*, *CXCL10*, *CXCL11* or *IFNB1* were among the DE genes specifically induced on IFN- γ +TL8-506 or Poly(I:C)+TL8-506 stimulation, respectively (figure 3D, online supplemental table 4). We have focused our analyses on cytokines and chemokines as readouts for cDC activation since we have observed strongest synergy in the induction of cytokines and chemokines by TL8-506 combinations compared with the expression of genes involved in co-stimulation and antigen presentation. However, TL8-506 combinations also upregulated other DC maturation markers including co-stimulatory molecules *CD80*, *CD83*, *CD86* and components of the antigen presentation machinery such as *TAP1*, *TAP2* and *HLA-DOB* (online supplemental figure S5A,B). The changes in gene expression in activated cDCs are likely regulated by both TLR and IFN signaling (online supplemental figure S6A,B). In summary, we demonstrate that tumor-derived cDCs from multiple indications respond to TL8-506 combinations and upregulate different relevant DC activation markers. In addition, the scRNA-seq analysis of treated tumor-derived cDCs revealed that the combination-specific induction of different cytokines

and chemokines was remarkably conserved between cord blood, blood and patient tumor cDCs.

TL8-506 combinations induce a Th1-supportive gene signature in human tumor-derived DCs

Since cDCs with an activated phenotype are present in different tumor indications (figure 4A,B, online supplemental figure S4A,B), we were interested in comparing the expression profile of treated tumor-derived cDCs to tumor cDCs activated *in situ* in human tumors. After four hours stimulation with TL8-506 combinations most treated cDCs clustered closely with the *in situ* activated DC population (figure 4C,D). Some of these treated cDCs fell into the *in situ* activated DC cluster and others were localized as an intermediate population between the cDC2 and the *in situ* activated DC cluster.

The fraction of unspliced versus spliced reads was recently employed to show a differentiation trajectory, referred to as a cell's velocity.²⁸ To estimate the likely directionality of transitions of stimulated tumor cDC subsets, we performed velocity analysis. Our results suggest that in response to TL8-506-based combinations activated tumor DCs are derived from immature cDCs (figure 4E). Compared with *in situ* activated cDCs present in cancer tissues, cDCs activated by TL8-506-based combinations showed increased expression of many DC activation markers including *IL12A*, *IL12B*, *CD40*, *IFNB1* and *IFNL1* (figure 4F,G), across the analyzed tumor indications (online supplemental figure S7A,B). In addition, tumor cDCs activated by TL8-506 combinations displayed higher expression of *CXCL9*, *CXCL10*, *CXCL11* and *CCL4*, chemokines associated with CD8⁺ T cell recruitment.^{5,44} In contrast, cDCs activated *in situ* by the tumor microenvironment showed increased expression of *CCL17* and *CCL22*, chemokines described to recruit CD4⁺ regulatory T cells.⁴⁵ Consistent with earlier reports, the highest levels of *IL12A* and *IL12B* were observed in the activated DC cluster, validating our readout to screen and select the best cDC activating compounds (figure 4H). In conclusion, our data show that most tumor-derived cDCs can be activated by TL8-506-based combinations. Activated cDCs generated by *ex vivo* stimulation acquired a phenotype that is associated with a Th1 response, displaying increased expression of *IL12A*, *IL12B*, *IFNB1*, *IFNL1*, *CD40* and CD8⁺ T cell chemokines when compared with cDCs activated *in situ* by the tumor microenvironment.

As transcript and protein levels do not necessarily correlate, we validated selected genes for which antibodies were available by intracellular flow cytometry. In agreement with our earlier observations (figure 2B,D), metastatic melanoma-derived, CRC-derived (figure 5A) and non-small cell lung cancer-derived (figure 5B) cDCs co-expressed intracellular TNF- α and CXCL10 proteins on IFN- γ +TL8-506 treatment. Treatment of tumor-derived cDC1s with Poly(I:C)+TL8-506 induced the co-expression of intracellular TNF- α and IFN- λ proteins, but not TNF- α and CXCL10 (figure 5A). The availability of sufficient patient-derived melanoma material allowed us to also

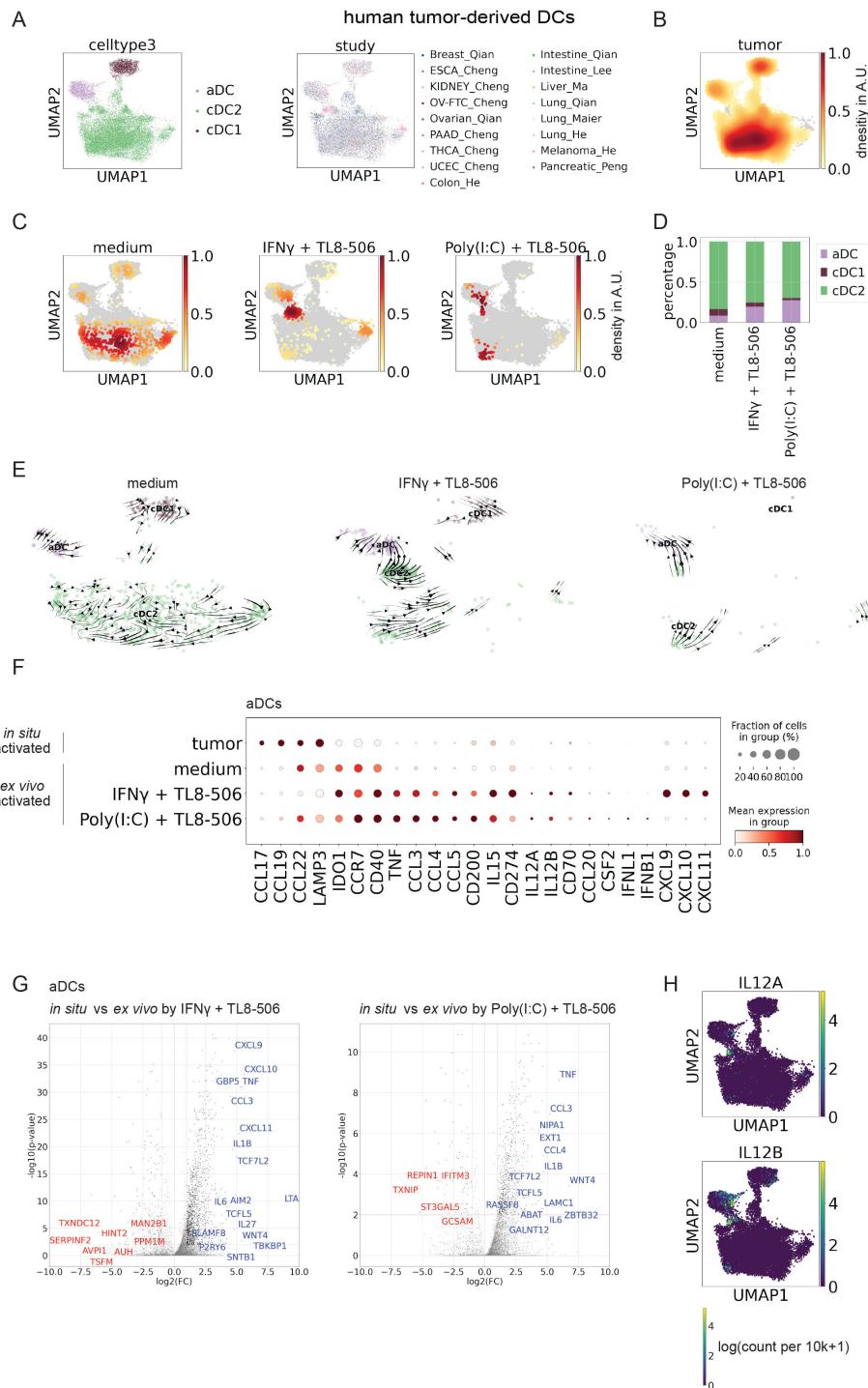


Figure 4 Human tumor-derived cDCs show an immunostimulatory phenotype associated with Th1 responses on stimulation with TL8-506 combinations. (A) UMAP of 18'651 human tumor-derived cDC1s, cDC2s and activated DCs (aDCs) profiled across different single-cell RNA-sequencing studies with each cell color-coded for cDC subset (left) and study (right). (B) Gaussian kernel density plot of human tumor-derived cDCs from integrated public studies, AU, arbitrary units. (C) Gaussian kernel density plot of human tumor-derived cDCs on treatment with TL8-506 combinations; AU, arbitrary units. (D) Quantification of activated DCs in patient tumor digests on treatment with TL8-506 combinations. (E) Velocity analysis of human tumor cDCs on treatment with TL8-506 combinations. (F) Fraction positive and mean expression of activation markers in *ex vivo* activated tumor DCs on treatment with TL8-506 combinations or *in situ* activated tumor DCs from integrated public studies. Mean expression was calculated across all the cells in the group and then scaled to a 0–1 range. (G) Volcano plots showing differentially expressed (DE) genes (blue: upregulated, red: downregulated) between *ex vivo* activated tumor DCs on treatment with TL8-506 combinations and *in situ* activated tumor DCs from integrated public studies. Top 20 DE genes scored by p-values and fold changes are labeled, Wilcoxon rank-sum test. Top 50 DE genes ranked by log₂ fold change (log₂FC) are listed in online supplemental table 4. (H) UMAP plots showing expression values of *IL12A* and *IL12B* in tumor cDCs across different studies in log(count per 10k+1). cDC, conventional DC; DC, dendritic cell; IFN, interferon; IL, interleukin.

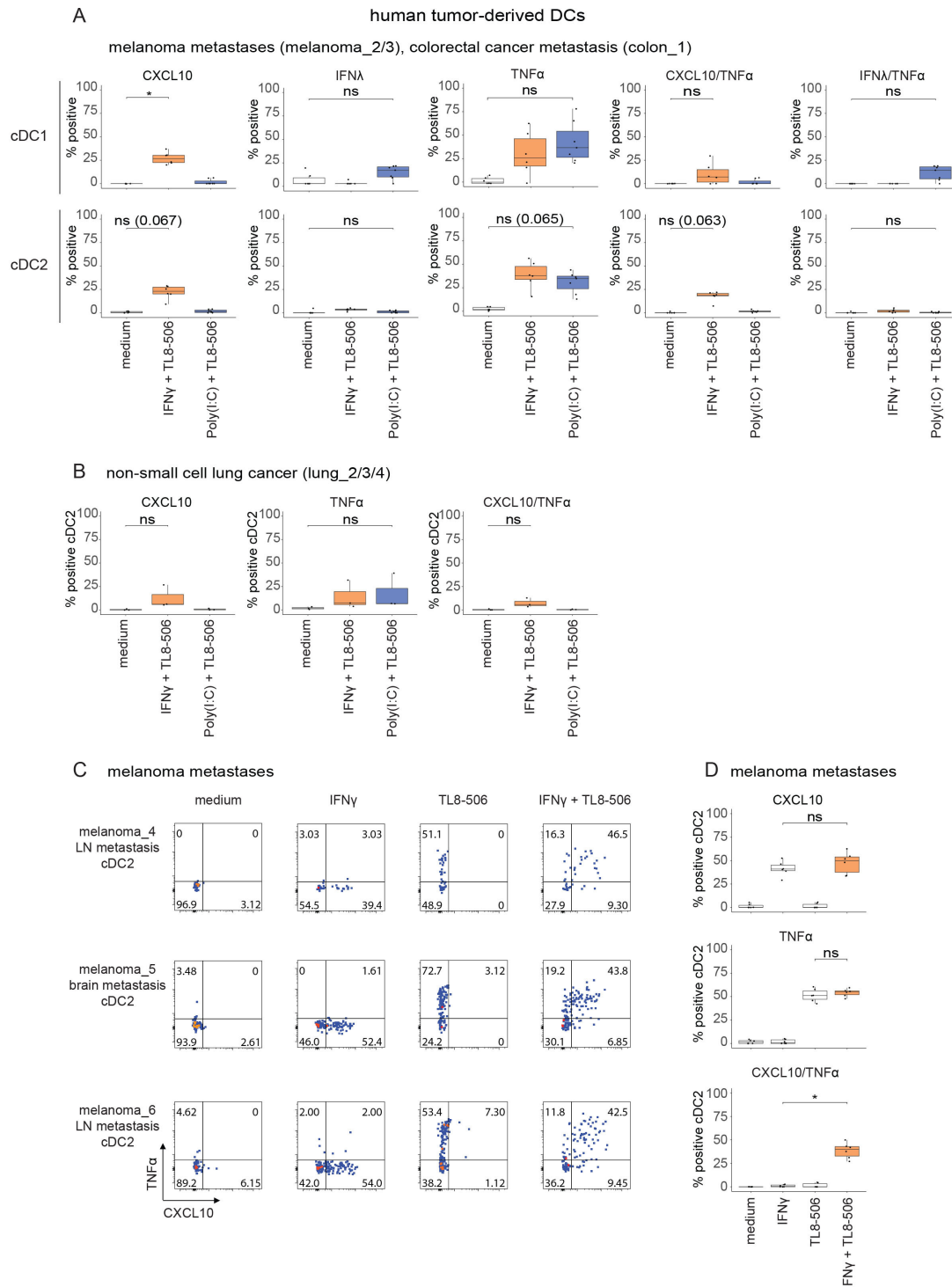


Figure 5 TL8-506-based combinations induce stimulus-specific cytokine protein expression in human tumor-derived cDCs. Tumor digests from patients with melanoma, CRC and lung cancer were treated with 1 μ M TL8-506+50'000 U/mL IFN- γ or 1 μ M TL8-506+10 μ g/mL Poly(I:C) for three hours. Intracellular cytokine staining was performed for CXCL10, IFN- λ and TNF- α . Protein expression in tumor-derived cDCs was analyzed by flow cytometry. (A) Quantification of indicated cytokine producing cDC1s and cDC2s from digested metastases of patients with melanoma and CRC on treatment with TL8-506 combinations, n=three donors, from three independent experiments. (B) Quantification of indicated cytokine expressing cDC2s in non-small cell lung cancer digests on treatment with TL8-506 combinations, n=three donors, from three independent experiments. (C) Flow cytometry plots of IFN- γ +TL8-506 or single agent treated cDC2s from digested melanoma lymph node (LN) and brain metastases showing the distribution of CXCL10 or/and TNF- α expressing cDC2s. Percentage of positive cells are indicated in the quadrants. (D) Quantification of CXCL10 or/and TNF- α expressing tumor-derived cDC2s from C, n=three donors, from three independent experiments. Statistics for A, B, D: Student's paired t-test, * $p \leq 0.03$, ns, not significant. The following concentrations were used for DC stimulation: 50'000 U/mL hIFN- γ , 10 μ g/mL Poly(I:C), 1 μ M TL8-506. cDC, conventional DC; CRC, colorectal cancer; DC, dendritic cell; IFN, interferon; TNF, tumor necrosis factor.

test the individual effects of TL8-506 and IFN- γ on tumor-derived cDCs. Consistent with our observations in blood cDCs, TL8-506 or IFN- γ by themselves did not induce the co-expression of intracellular TNF- α and CXCL10 proteins in tumor-derived cDCs (figure 5C,D). In conclusion, our data confirm that TL8-506-based combinations induce the stimulus-specific protein expression of cytokines and chemokines in tumor-derived cDCs.

DC activation by Poly(I:C)+TL8-506 results in enhanced T cell activation, DC and T cell recruitment

The previous results suggest that selected cytokines and chemokines are produced by tumor-derived cDCs in response to TL8-506-based combinations. To better understand the functional relevance of the factors secreted by tumor-derived cDCs on stimulation with TL8-506-based combinations, we performed co-culture and migration assays. We sorted cord blood cDCs as cDCs from patient tumor material were insufficient in numbers to perform functional assays and the response of cord blood cDCs to TL8-506 combinations was comparable to those of tumor-derived cDCs (figures 1E and 3B).

First, we assessed the effects of activated cDCs on Th1 differentiation using the production of IFN- γ as a proxy. Sorted cDCs were treated for 18 hours and the stimuli were removed by several washing steps. Activated cDCs were then co-cultured with allogeneic naive T cells and after four days the IFN- γ concentrations in the supernatant were measured. cDCs stimulated with Poly(I:C)+TL8-506 induced the highest IFN- γ concentrations among the tested stimuli with a 140-fold increase compared with unstimulated cDCs (figure 6A). In addition, we investigated the induction of other Th-associated cytokines in DC/T cell co-cultures such as IL-4 and IL-10 and did not observe their secretion (online supplemental figure S8).

Next, we analyzed how the different chemokines induced by TL8-506-based combinations impact the recruitment of DCs. Supernatants of stimulated cDCs were placed in the lower compartment of a transwell. Untreated cord blood DCs were added into the transwell inserts and DC migration was measured after three hours by quantification of cDCs in the lower compartment by flow cytometry. Treatment of cDCs with Poly(I:C)+TL8-506 induced a 20-fold higher recruitment of cDCs compared with untreated cDCs (figure 6B). This was likely related to our observation that Poly(I:C)+TL8-506 synergized in the secretion of CCL3, CCL4 and CCL20, a set of chemokines described to promote DC migration.^{46,47} Since the supernatants also contained the TLR agonists, it cannot be excluded that the agonists have influenced the migratory capacity of DCs in the presence of cytokines and chemokines released by activated cDCs.

T cell migration was studied using a three-dimensional (3D) tissue culture platform in which activated CD8⁺ cells were allowed to transmigrate through an artificial endothelial vessel and collagen layer towards supernatants of stimulated cDCs. Migrated T cells were quantified after 48 hours by imaging of the collagen layer. Poly(I:C)+TL8-506

treatment of cDCs led to a ten-fold increase in CD8⁺ T cell recruitment when compared with untreated cDCs (figure 6C,D). In contrast, IFN- γ +TL8-506 failed to induce the recruitment of significant numbers of CD8⁺ T cells. IFN- γ +TL8-506 stimulation induced the strongest CXCL10 secretion while Poly(I:C)+TL8-506 treatment induced the highest CCL4 and TNF- α release in cDCs among the tested combinations (online supplemental figure S9A). CXCL10, CCL4 and TNF- α are all associated with CD8⁺ T cell chemotaxis.^{48–50} Hence, it is possible that the CCL4/TNF- α axis was more efficient in attracting CD8⁺ T cells in our 3D system. Blocking of CCL4 in cDC supernatants had no impact on CD8⁺ T cell migration suggesting that the recruitment depends on additional chemokines (online supplemental figure S9B). However, recombinant CCL4 and TNF- α at concentrations present in supernatants of Poly(I:C)+TL8-506 treated cDCs were sufficient to induce CD8⁺ T cell migration (online supplemental figure S9C). In summary, factors released by cDCs in response to Poly(I:C)+TL8-506 stimulation increased the recruitment of cDCs, CD8⁺ T cells and T cell activation. Hence, treatment of patients with cancer with TLR8 agonist-based combinations may help to inflame tumors, enhance tumor specific CD8⁺ T cell activities and boost anticancer immunity in patients.

DISCUSSION

Most cDCs in human tumors show a non-activated phenotype.^{7,8} Two potential non-mutually exclusive explanations have been proposed in the literature: (1) Lack of cDC activating signals in the tumor; (2) the tumor micro-environment releases factors that preclude the differentiation of immunostimulatory cDCs. We stimulated human tumor cDCs derived from different cancer indications with TL8-506-based combinations, which induced the strongest activation of cord blood and blood cDCs among the tested treatments. We found that a majority of human tumor-derived cDCs were activated by TL8-506-based combinations *ex vivo*. Hence, our data indicate that most tumor-derived cDCs are responsive to activating signals. In accordance, transcriptome analysis revealed no major differences between cDCs present in healthy tissues and different cancer indications.

Low numbers of cDCs with an activated phenotype are observed in different human tumor indications. These *in situ* activated cDCs are characterized by the expression of *CCL17*, *CCL19* and *CCL22*, chemokines associated with CD4⁺ regulatory T cell recruitment.^{44,45} They also show increased expression of both co-stimulatory and co-inhibitory molecules such as *CD40* and *CD274* when compared with non-activated cDCs.⁷ However, no or only very few transcripts for factors associated with anti-tumor responses were detected including *IL12A*, *IL12B* and *IFNBI*. Interestingly, human tumor cDCs activated by TL8-506 combinations showed increased expression of *IL12A*, *IL12B*, *IFNBI*, chemokines for CD8⁺ T cells including *CXCL9*, *CXCL10* and *CCL4* but decreased

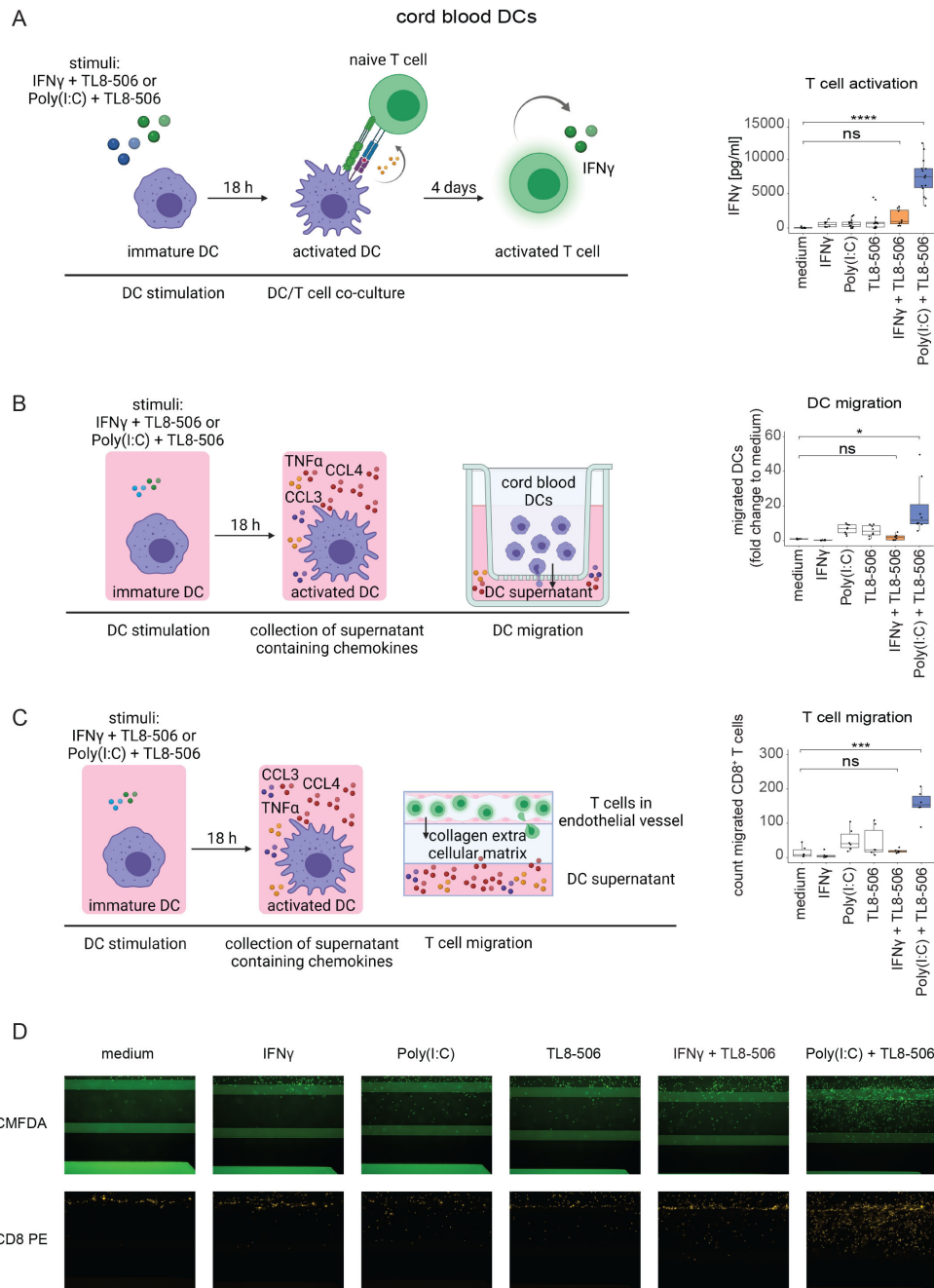


Figure 6 Poly(I:C)+TL8-506 stimulated cord blood cDCs induce T cell activation, DC and T cell recruitment. The experimental set-up for the functional assays is shown on the left. (A) Sorted cord blood cDC2s were stimulated with the indicated compounds for 18 hours. Treated cDC2s were washed and co-cultured with allogeneic naive T cells for four days. IFN- γ concentrations in the supernatant were determined by ELISA as a readout for T cell activation. IFN- γ concentrations are shown on the right, n=three batches of cord blood from mixed donors, six T cell donors, from four independent experiments. (B) Sorted cord blood cDC2s were stimulated with the indicated compounds for 18 hours. The supernatants were collected and placed into the lower compartment of a transwell. Untreated cord blood DCs were added into the transwell insert and allowed to migrate for three hours. Fold change to medium of migrated cord blood cDC1s+cDC2s is depicted on the right, n=four batches of cord blood from mixed donors, from four independent experiments. (C) Sorted cord blood cDC2s were stimulated with the indicated compounds for 18 hours. The supernatants were collected and placed into the bottom channel of a three-dimensional tissue culture device. Activated CD8 $^+$ T cells were labeled with CMFDA and added to the top channel that was coated with an artificial endothelial vessel. Migrated T cells were detected after 48 hours by imaging of the collagen layer that separated the two channels. Cell counts of migrated CD8 $^+$ T cells are shown on the right, n=two batches of cord blood from mixed donors, three T cell donors, from three independent experiments. (D) Representative microscopy images of CD8 $^+$ T cell migration described in C using the Operetta system at 10x magnification. One-way analysis of variance was used for statistical analysis, * $p \leq 0.03$, *** $p \leq 0.0002$, **** $p \leq 0.0001$, ns, not significant. The following concentrations were used for DC stimulation: 50'000 U/mL huIFN- γ , 10 μ g/mL Poly(I:C), 1 μ M TL8-506. Illustrations were created with BioRender.com. cDC, conventional DC; DC, dendritic cell; IFN, interferon; TNF, tumor necrosis factor.

expression of *CCL17*, *CCL19* and *CCL22* when compared with in situ activated tumor cDCs. Functional assays using in vitro activated cord blood cDCs confirmed that cDC-derived factors mediated CD8⁺ T cell recruitment and activation. In summary, our data indicate that inadequate or insufficient levels of activating signals are present in the tumor to induce proinflammatory factors associated with Th1 responses in cDCs. Importantly, TL8-506-based combinations were sufficient to induce a Th1-like phenotype in tumor cDCs even though tumor cells or the tumor microenvironment might release suppressive factors that counteract DC activation (online supplemental figure S10A,B). Future experiments will be required to explore the effects of in situ and ex vivo activated tumor DCs on T cell activation and recruitment in more detail.

In patients, it is possible that additional cells contribute to the proinflammatory effects of TL8-506-based combinations. TLR3 and TLR8 are preferentially, but not exclusively expressed on cDCs while IFN- γ receptors (IFNGRs) are ubiquitously expressed.⁵¹ Macrophages express both TLR8 and IFNGRs.⁵² Tumor-derived macrophages upregulated *CXCL10* and *TNF- α* expression on IFN- γ -TL8-506 treatment, but failed to induce *IL12A*, *IL12B*, *IFNB1* or *IFNL1* on stimulation with TL8-506 combinations (online supplemental figure S11A,B).

Different human cDC sources have been explored for drug screenings to predict treatment effects on human tumor cDCs due to their scarcity.^{53,54} We tested the usefulness of in vitro differentiated cord blood and blood cDCs that can be isolated in greater numbers to predict the response of tumor cDCs. Cord blood cDC1s and cDC2s formed well separated clusters in scRNA-seq analyses despite the fact that cord blood cDC1s expressed some cDC2-specific markers and vice versa. Using different readouts, we found that the response of in vitro differentiated cord blood and blood cDCs to different stimuli was strikingly similar compared with tumor-derived cDCs although the cultures contained other cell types that might have influenced the activation of cDCs (online supplemental figure S12A–C). In a stimulus-specific manner, IFN- λ induced *CXCL10* production, Poly(I:C) induced IFN- λ expression and TL8-506 treatment resulted in *TNF- α* expression in cord blood, blood and tumor-derived cDCs. Surprisingly, only the stimulation with Poly(I:C)+TL8-506 but not IFN- γ +TL8-506 led to IFN- β expression in cord blood and tumor cDCs. However, it is possible that the experimental set-up influenced the IFN- β expression as the induction of IFN- β by TLR8 agonists in human DCs was inconsistent in previous studies.^{55,56} We conclude that in vitro differentiated cord blood and peripheral blood cDCs are useful surrogates to test the ability of drug candidates to activate human tumor-associated cDCs.

One focus of the study was also to compare treatment responses of human cDC1s and cDC2s. Although activated cDC1 and cDC2 clustered together and had similar overall gene expression profile, selected genes were differentially induced. As previously described in the literature, IFN- λ was selectively induced by Poly(I:C) in cDC1s.¹⁷

Poly(I:C) consistently showed stronger effects on cDC1s compared with cDC2s, which might be explained by the higher TLR3 expression in cDC1s.²¹ In contrast, we did not identify any cytokine that was selectively induced in cDC2s on stimulation with TL8-508 combinations. This highlights the importance of differential PRR expression in human cDCs and how it may guide the selection of appropriate agonists to target different cDC subsets.

TLR3 agonists, TLR8 agonists and IFN- γ are currently being tested for cancer treatment in different clinical trials.^{57,58} The results from past clinical trials have been rather disappointing showing no significant improvement in patient outcome, probably due to systemic toxicities and the lack of preferential accumulation in the tumor of untargeted molecules. cDC-targeted or/and tumor-targeted versions of current TLR3 and TLR8 agonists in development might improve treatment efficacy while reducing toxicity. To exploit synergistic effects in cDC activation, dual agonists can be designed to activate both TLR3 and TLR8 to increase their potency specifically in cDCs because they co-express TLR3 and TLR8. In addition, cDC activation in combination with radiotherapy or immune checkpoint inhibition has shown promising results in many preclinical models and may further improve treatment efficacy. Our study provides insights for the rational combination of cDC agonists to optimally activate human tumor cDCs and improve antitumor immunity in patients with cancer.

Author affiliations

¹Roche Pharma Research and Early Development, Roche Innovation Center Zurich, Schlieren, Switzerland

²Roche Pharma Research and Early Development, Roche Innovation Center Basel, Basel, Switzerland

³Roche Pharma Research and Early Development, Roche Innovation Center Munich, Penzberg, Germany

⁴Department of Dermatology, University Hospital Zurich, Zurich, Switzerland

⁵Institute of Experimental Immunology, University of Zurich, Zurich, Switzerland

Twitter Bhavesh Soni @bsoni08 and Maries van den Broek @vandenBroek_Lab

Acknowledgements We thank Professor Christian Münz for the scientific inputs. We thank Thuy Trinh Nguyen for her support in T cell migration assays. Many thanks to Ramona Schlenker, Marisa Mariani and Emilio Yanguuez for their support in single-cell RNA-sequencing. We thank Regula Buser for the fluorescent labeling of antibodies. We thank Said Aktas for his input for the NanoString and statistical analyses. We want to thank Eva Sum, Floriana Cremasco, Philipp Fröbel and Lucia Campos for the helpful discussions. Finally, we thank all our colleagues from Roche for their continuous support through all phases of this project.

Contributors Concept and experimental design: MH, SC, IM, MvdB, SG. Acquisition of data: MH, YP, CW, LK. Data analysis and interpretation: MH, BS, PCS, MvdB, SG. Assay development: MH, TH, IM, CW, DDS. Provision of study materials: MPL, RD. Writing, review and/or revision of the manuscript: MH, BS, PCS, SC, IM, CT, MB, PU, MPL, MvdB, SG. Study supervision: MvdB, SG. Guarantor: SG.

Funding This project was funded by Roche.

Competing interests All authors, except MPL, RD and MvdB are employees of Roche.

Patient consent for publication Not applicable.

Ethics approval This study involves human participants and was approved by Business Administration System for Ethics Committees BASEC-Nr: 2020-01208, BASEC-Nr: 2017-00494, and BASEC-Nr: 2016-02013. Participants gave informed consent to participate in the study before taking part.

Provenance and peer review Not commissioned; externally peer reviewed.

Data availability statement Single-cell RNA-sequencing data are available in a public, open access repository. All other data relevant to the study are included in the article or uploaded as supplementary information. Single-cell RNA-sequencing data are stored at <https://www.ebi.ac.uk/arrayexpress>: Single-cell RNA-seq of human tumor digests treated with Toll-like receptor agonists and interferons against untreated controls (E-MTAB-11734), Single-cell RNA-seq of human blood dendritic cells from buffy coats and in vitro differentiated dendritic cells from cord blood CD34+ stem cells (E-MTAB-11735) and at <https://zenodo.org>: Integration of single-cell RNA-sequencing data across tissues and cancer types towards immune cell characterization (<https://doi.org/10.5281/zenodo.6514005>).

Supplemental material This content has been supplied by the author(s). It has not been vetted by BMJ Publishing Group Limited (BMJ) and may not have been peer-reviewed. Any opinions or recommendations discussed are solely those of the author(s) and are not endorsed by BMJ. BMJ disclaims all liability and responsibility arising from any reliance placed on the content. Where the content includes any translated material, BMJ does not warrant the accuracy and reliability of the translations (including but not limited to local regulations, clinical guidelines, terminology, drug names and drug dosages), and is not responsible for any error and/or omissions arising from translation and adaptation or otherwise.

Open access This is an open access article distributed in accordance with the Creative Commons Attribution Non Commercial (CC BY-NC 4.0) license, which permits others to distribute, remix, adapt, build upon this work non-commercially, and license their derivative works on different terms, provided the original work is properly cited, appropriate credit is given, any changes made indicated, and the use is non-commercial. See <http://creativecommons.org/licenses/by-nc/4.0/>.

ORCID iDs

Mi He <http://orcid.org/0000-0002-8271-6672>

Reinhard Dummer <http://orcid.org/0000-0002-2279-6906>

Maries van den Broek <http://orcid.org/0000-0002-9489-3692>

REFERENCES

- Banchereau J, Steinman RM. Dendritic cells and the control of immunity. *Nature* 1998;392:245–52.
- Hildner K, Edelson BT, Purtha WE, et al. Batf3 deficiency reveals a critical role for CD8alpha+ dendritic cells in cytotoxic T cell immunity. *Science* 2008;322:1097–100.
- Roberts EW, Broz ML, Binnewies M, et al. Critical role for CD103(+)/CD141(+) dendritic cells bearing CCR7 for tumor antigen trafficking and priming of T cell immunity in Melanoma. *Cancer Cell* 2016;30:324–36.
- Garris CS, Arlauckas SP, Kohler RH, et al. Successful anti-PD-1 cancer immunotherapy requires T Cell-Dendritic cell crosstalk involving the cytokines IFN- γ and IL-12. *Immunity* 2018;49:1148–61.
- Chow MT, Ozga AJ, Servis RL, et al. Intratumoral activity of the CXCR3 chemokine system is required for the efficacy of anti-PD-1 therapy. *Immunity* 2019;50:1498.
- Tran Janco JM, Lamichhane P, Karyampudi L, et al. Tumor-Infiltrating dendritic cells in cancer pathogenesis. *J Immunol* 2015;194:2985–91.
- Maier B, Leader AM, Chen ST, et al. A conserved dendritic-cell regulatory program limits antitumor immunity. *Nature* 2020;580:257–62.
- Cheng S, Li Z, Gao R, et al. A pan-cancer single-cell transcriptional atlas of tumor infiltrating myeloid cells. *Cell* 2021;184:792–809.
- Sancho D, Joffre OP, Keller AM, et al. Identification of a dendritic cell receptor that couples sensing of necrosis to immunity. *Nature* 2009;458:899–903.
- Canton J, Blees H, Henry CM, et al. The receptor DNCR-1 signals for phagosomal rupture to promote cross-presentation of dead-cell-associated antigens. *Nat Immunol* 2021;22:140–53.
- Villani A-C, Satija R, Reynolds G, et al. Single-cell RNA-seq reveals new types of human blood dendritic cells, monocytes, and progenitors. *Science* 2017;356:aah4573. doi:10.1126/science.aah4573
- Dudziak D, Kamphorst AO, Heidkamp GF, et al. Differential antigen processing by dendritic cell subsets in vivo. *Science* 2007;315:107–11.
- Eisenbarth SC. Dendritic cell subsets in T cell programming: location dictates function. *Nat Rev Immunol* 2019;19:89–103.
- Noubade R, Majri-Morrison S, Tarbell KV. Beyond cDC1: emerging roles of DC crosstalk in cancer immunity. *Front Immunol* 2019;10:1014.
- Nizzoli G, Krietsch J, Weick A, et al. Human CD1c+ dendritic cells secrete high levels of IL-12 and potentially prime cytotoxic T-cell responses. *Blood* 2013;122:932–42.
- Truxova I, Kasikova L, Hensler M, et al. Mature dendritic cells correlate with favorable immune infiltrate and improved prognosis in ovarian carcinoma patients. *J Immunother Cancer* 2018;6:139.
- Hubert Met al. IFN-III is selectively produced by cdc1 and predicts good clinical outcome in human breast cancer. *Cancer Immunol Res* 2020;8:70.
- Oba T, Long MD, Keler T, et al. Overcoming primary and acquired resistance to anti-PD-L1 therapy by induction and activation of tumor-residing cDC1s. *Nat Commun* 2020;11:5415.
- Roselli E, Araya P, Núñez NG, et al. TLR3 activation of intratumoral CD103+ dendritic cells modifies the tumor infiltrate conferring anti-tumor immunity. *Front Immunol* 2019;10:503.
- Gautier G, Humbert M, Deauvieu F, et al. A type I interferon autocrine-paracrine loop is involved in Toll-like receptor-induced interleukin-12p70 secretion by dendritic cells. *J Exp Med* 2005;201:1435–46.
- Hémont C, Neel A, Heslan M, et al. Human blood mDC subsets exhibit distinct TLR repertoire and responsiveness. *J Leukoc Biol* 2013;93:599–609.
- Kratky W, Reis e Sousa C, Oxenius A, et al. Direct activation of antigen-presenting cells is required for CD8+ T-cell priming and tumor vaccination. *Proc Natl Acad Sci U S A* 2011;108:17414–9.
- Napolitani G, Rinaldi A, Bertoni F, et al. Selected Toll-like receptor agonist combinations synergistically trigger a T helper type 1-polarizing program in dendritic cells. *Nat Immunol* 2005;6:769–76.
- Lövgren T, Sarhan D, Truxová I, et al. Enhanced stimulation of human tumor-specific T cells by dendritic cells matured in the presence of interferon- γ and multiple toll-like receptor agonists. *Cancer Immunol Immunother* 2017;66:1333–44.
- Zheng GXY, Terry JM, Belgrader P, et al. Massively parallel digital transcriptional profiling of single cells. *Nat Commun* 2017;8:14049.
- Mädler SC, Julien-Laferrriere A, Wyss L, et al. Besca, a single-cell transcriptomics analysis toolkit to accelerate translational research. *NAR Genom Bioinform* 2021;3:lqab102.
- Traag VA, Waltman L, van Eck NJ. From Louvain to Leiden: guaranteeing well-connected communities. *Sci Rep* 2019;9:5233.
- La Manno G, Soldatov R, Zeisel A, et al. RNA velocity of single cells. *Nature* 2018;560:494–8.
- Bergen V, Lange M, Peidli S, et al. Generalizing RNA velocity to transient cell states through dynamical modeling. *Nat Biotechnol* 2020;38:1408–1414.
- Vignali DAA, Kuchroo VK. IL-12 family cytokines: immunological playmakers. *Nat Immunol* 2012;13:722–8.
- Valenzuela J, Schmidt C, Mescher M. The roles of IL-12 in providing a third signal for clonal expansion of naive CD8 T cells. *J Immunol* 2002;169:6842–9.
- Lichtenegger FS, Mueller K, Otte B, et al. CD86 and IL-12p70 are key players for T helper 1 polarization and natural killer cell activation by Toll-like receptor-induced dendritic cells. *PLoS One* 2012;7:e44266.
- Qian J, Olbrecht S, Boeckx B, et al. A pan-cancer blueprint of the heterogeneous tumor microenvironment revealed by single-cell profiling. *Cell Res* 2020;30:745–62.
- Lee H-O, Hong Y, Etilioglu HE, et al. Lineage-dependent gene expression programs influence the immune landscape of colorectal cancer. *Nat Genet* 2020;52:594–603.
- Ma L, Hernandez MO, Zhao Y, et al. Tumor cell biodiversity drives microenvironmental reprogramming in liver cancer. *Cancer Cell* 2019;36:418–30.
- Peng J, Sun B-F, Chen C-Y, et al. Author correction: single-cell RNA-seq highlights intra-tumoral heterogeneity and malignant progression in pancreatic ductal adenocarcinoma. *Cell Res* 2019;29:777.
- Cillo AR, Kürten CHL, Tabib T, et al. Immune landscape of viral- and carcinogen-driven head and neck cancer. *Immunity* 2020;52:183–99.
- Martin JC, Chang C, Boschetti G, et al. Single-cell analysis of Crohn's disease lesions identifies a pathogenic cellular module associated with resistance to anti-TNF therapy. *Cell* 2019;178:1493–508.
- Smillie CS, Biton M, Ordovas-Montanes J, et al. Intra- and Inter-cellular rewiring of the human colon during ulcerative colitis. *Cell* 2019;178:714–30.
- Ramachandran P, Dobie R, Wilson-Kanamori JR, et al. Resolving the fibrotic niche of human liver cirrhosis at single-cell level. *Nature* 2019;575:512–8.
- Raredon MSB, Adams TS, Suhail Y, et al. Single-cell connectomic analysis of adult mammalian lungs. *Sci Adv* 2019;5:eaaw3851.
- Kotliarov Y, Sparks R, Martins AJ, et al. Broad immune activation underlies shared set point signatures for vaccine responsiveness in



- healthy individuals and disease activity in patients with lupus. *Nat Med* 2020;26:618–29.
- 43 Madisson E, Wilbrey-Clark A, Miragaia RJ, *et al.* scRNA-seq assessment of the human lung, spleen, and esophagus tissue stability after cold preservation. *Genome Biol* 2019;21:1.
- 44 Hoch T, Schulz D, Eling N, *et al.* Multiplexed imaging mass cytometry of the chemokine milieu in melanoma characterizes features of the response to immunotherapy. *Sci Immunol* 2022;7:eabk1692.
- 45 Rapp M, Wintergerst MWM, Kunz WG, *et al.* CCL22 controls immunity by promoting regulatory T cell communication with dendritic cells in lymph nodes. *J Exp Med* 2019;216:1170–81.
- 46 Williford J-M, Ishihara J, Ishihara A, *et al.* Recruitment of CD103⁺ dendritic cells via tumor-targeted chemokine delivery enhances efficacy of checkpoint inhibitor immunotherapy. *Sci Adv* 2019;5:eaay1357.
- 47 Spranger S, Bao R, Gajewski TF. Melanoma-intrinsic β -catenin signalling prevents anti-tumour immunity. *Nature* 2015;523:231–61.
- 48 Liu J, Li F, Ping Y, *et al.* Local production of the chemokines CCL5 and CXCL10 attracts CD8⁺ T lymphocytes into esophageal squamous cell carcinoma. *Oncotarget* 2015;6:24978–89.
- 49 Castellino F, Huang AY, Altan-Bonnet G, *et al.* Chemokines enhance immunity by guiding naive CD8⁺ T cells to sites of CD4⁺ T cell-dendritic cell interaction. *Nature* 2006;440:890–5.
- 50 Jaczewska J, Abdulreda MH, Yau CY, *et al.* TNF- α and IFN- γ promote lymphocyte adhesion to endothelial junctional regions facilitating transendothelial migration. *J Leukoc Biol* 2014;95:265–74.
- 51 Iwasaki A, Medzhitov R. Toll-like receptor control of the adaptive immune responses. *Nat Immunol* 2004;5:987–95.
- 52 Schroder K, Hertzog PJ, Ravasi T, *et al.* Interferon-gamma: an overview of signals, mechanisms and functions. *J Leukoc Biol* 2004;75:163–89.
- 53 Balan S, Ollion V, Colletti N, *et al.* Human XCR1⁺ dendritic cells derived in vitro from CD34⁺ progenitors closely resemble blood dendritic cells, including their adjuvant responsiveness, contrary to monocyte-derived dendritic cells. *J Immunol* 2014;193:1622–35.
- 54 Lee J, Breton G, Oliveira TYK, *et al.* Restricted dendritic cell and monocyte progenitors in human cord blood and bone marrow. *J Exp Med* 2015;212:385–99.
- 55 Mäkelä SM, Osterlund P, Julkunen I. TLR ligands induce synergistic interferon- β and interferon- λ 1 gene expression in human monocyte-derived dendritic cells. *Mol Immunol* 2011;48:505–15.
- 56 Larangé A, Antonios D, Pallardy M, *et al.* TLR7 and TLR8 agonists trigger different signaling pathways for human dendritic cell maturation. *J Leukoc Biol* 2009;85:673–83.
- 57 Chiang CL-L, Kandalafi LE. In vivo cancer vaccination: which dendritic cells to target and how? *Cancer Treat Rev* 2018;71:88–101.
- 58 Ni L, Lu J. Interferon gamma in cancer immunotherapy. *Cancer Med* 2018;7:4509–16.

Supplementary Materials

Table 1. Antibodies for flow cytometry

Target	Fluorophore	Company	Catalog number	Clone
FACSAria III panel for sorting of cord blood DCs				
CD141	BV711	BD	563155	1A4
CD1c	PE-Cy7	Biolegend	331516	L161
CD14	PerCP-Cy5.5	Biolegend	325622	HCD14
CLEC9A	APC	Biolegend	353806	8F9
CD45	AF700	Biolegend	304024	HI30
Dead Cell Stain	Near-IR	Life Technologies	L34976	
FACSAria III panel for enrichment of DCs from tumor digests				
CD45	BV510	Biolegend	304036	HI30
CD3	AF488	Biolegend	317310	OKT3
Dead Cell Stain	Near-IR	Life Technologies	L34976	
LSRFortessa panel for cytokine expression in blood or tumor-derived DCs				
CD11c	BV421	Biolegend	301628	3.9
CD45	BV510	Biolegend	304036	HI30
TNF α	BV605	Biolegend	502936	MAB11
CD56	BV650	Biolegend	318344	HCD56
CD16	BV711	Biolegend	302044	3G8
IFN λ	AF488*	R&D Systems	MAB15981-500	247801
CD14	PerCP-Cy5.5	Biolegend	325622	HCD14
CXCL9	PE	Biolegend	519504	J034D6
CXCL10	PE	Biolegend	357904	J1015E10
CD3	PE-Cy5	BD	555341	HIT3a
CD1c	PE-Cy7	Biolegend	331516	L161
CLEC9A	APC	Biolegend	353806	8F9
CD19	AF700	Biolegend	302226	HIB19
HLA-DR	BUV395	BD	564040	G46-6
Dead Cell Stain	Near-IR	Life Technologies	L34976	

FACSymphony A5 panel for cytokine expression in blood or tumor-derived DCs				
CD3	BUV395	BD	740283	HIT3a
CD19	BUV395	BD	563551	SJ25C1
HLA-DR	BUV496	BD	741157	Tu39
CD16	BUV615	BD	750572	3G8
CD56	BUV661	BD	750478	NCAM16.2
CD45	BUV805	BD	612891	HI30
TNF α	BV605	Biologend	502936	MAB11
CD14	BV650	BD	740633	M ϕ P9
IFN λ	AF488*	R&D Systems	MAB15981-500	247801
CXCL10	PE	Biologend	519504	J034D6
CD68	PE-eFluor 610	invitrogen	61-0689-42	Y1/82A
CD1c	PE-Cy7	Biologend	331516	L161
CLEC9A	APC	Biologend	353806	8F9
CD11c	AF700	Biologend	337220	Bu15
Dead Cell Stain	Near-IR	Life Technologies	L34976	

* anti-IFN λ antibodies in AF488: in-house labeling (Invitrogen, #A30005)

Table 2. Overview of scRNA-seq studies

Study_name	Tissue_type	Status	Study
Ovarian_Qian	Ovarian	Solid tumor - Cancer	Qian <i>et al.</i>
OV-FTC_Cheng	Ovarian	Solid tumor - Cancer	Cheng <i>et al.</i>
Lung_Qian	Lung	Solid tumor - Cancer	Qian <i>et al.</i>
Breat_Qian	Breast	Solid tumor - Cancer	Qian <i>et al.</i>
THCA_Cheng	Thyroid Carcinoma (THCA)	Solid tumor - Cancer	Cheng <i>et al.</i>
ESCA_Cheng	Esophageal Carcinoma (ESCA)	Solid tumor - Cancer	Cheng <i>et al.</i>
Kidney_Cheng	Kidney cancer	Solid tumor - Cancer	Cheng <i>et al.</i>
PAAD_Cheng	Pancreatic adenocarcinoma (PAAD)	Solid tumor - Cancer	Cheng <i>et al.</i>
UCEC_Cheng	Uterine Corpus Endometrial Carcinoma (UCEC)	Solid tumor - Cancer	Cheng <i>et al.</i>
HN_Cillo	Head and Neck cancer	Solid tumor - Cancer	Cillo <i>et al.</i>
Intestine_Qian	Intestine/Colorectal	Solid tumor - Cancer	Qian <i>et al.</i>
Intestine_Lee	Intestine/Colorectal	Solid tumor - Cancer	Lee <i>et al.</i>
Liver_Ma	Liver	Solid tumor - Cancer	Ma <i>et al.</i>
Lung_Maier	Lung	Solid tumor - Cancer	Maier <i>et al.</i>
Pancreatic_Peng	Pancreatic cancer	Solid tumor - Cancer	Peng <i>et al.</i>
PBMC_Cillo	Head and Neck PBMC - cancer	Blood sample from cancer patients	Cillo <i>et al.</i>
PBMC_Cillo_nc	Head and Neck PBMC - healthy	Blood sample from healthy donors	Cillo <i>et al.</i>
Intestine_Smillie	Intestine	Non-cancer	Smillie <i>et al.</i>
Pancreatic_Peng_nc	Pancreas	Non-cancer	Peng <i>et al.</i>
Lung_Raredon	Lung	Non-cancer	Raredon <i>et al.</i>
Lung_Madisooson	Lung	Non-cancer	Madisooson <i>et al.</i>
Tonsils_Cillo	Tonsils	Non-cancer	Cillo <i>et al.</i>
PBMC_Kotliarov	PBMC	Non-cancer	Kotliarov <i>et al.</i>
Liver_Ramachandran	Liver	Non-cancer	Ramachandran <i>et al.</i>
Intestine_Martin	Intestine	Non-cancer	Martin <i>et al.</i>
CBDCs_He	CBDCs	Cord blood sample	He <i>et al.</i>
PBMC_He	PBMC	Blood sample	He <i>et al.</i>
Lung_He	Lung	Solid tumor - Cancer, IFN γ +TL8-506 and Poly(I:C)+TL8-506 treated	He <i>et al.</i>
Colon_He	Colon	Solid tumor - Cancer, IFN γ +TL8-506 and Poly(I:C)+TL8-506 treated	He <i>et al.</i>
Melanoma_He	Melanoma	Solid tumor - Cancer, IFN γ +TL8-506 treated	He <i>et al.</i>

Table 3. Parameters for the filtering of high-quality cells in scRNA-seq studies

Study_name	standard_min_genes	standard_min_cells	standard_min_counts	standard_n_genes	standard_percent_mito	standard_max_counts
Ovarian_Qian	800	10	600	6000	0.1	55000
OV-FTC_Cheng	500	10	1000	6000	0.15	50000
Lung_Qian	600	10	1000	6000	0.15	70000
Breat_Qian	400	10	800	5900	0.03	70000
THCA_Cheng	500	10	1000	6000	0.15	50000
ESCA_Cheng	500	10	1000	6000	0.15	50000
Kidney_Cheng	500	10	1000	6000	0.15	50000
PAAD_Cheng	500	10	1000	6000	0.15	50000
UCEC_Cheng	500	10	1000	6000	0.15	50000
HN_Cillo	400	10	1200	7000	0.3	70000
Intestine_Qian	800	10	1200	6000	0.1	55000
Intestine_Lee	500	20	1000	6000	0.1	70000
Liver_Ma	500	30	1500	7000	0.15	60000
Lung_Maier	800	20	1500	5000	0.1	30000
Pancreatic_Peng	500	20	1000	8000	0.1	80000
PBMC_Cillo	600	10	1200	5000	0.15	40000
PBMC_Cillo_nc	600	10	1200	5000	0.15	40000
Intestine_Smillie	800	30	2000	8000	0.2	100000
Pancreatic_Peng_nc	800	30	2000	8000	0.2	100000
Lung_Raredon	700	20	1000	8000	0.15	60000
Lung_Madissoon	700	20	1000	8000	0.1	80000
Tonsils_Cillo	400	10	1700	7000	0.1	70000
PBMC_Kotliarov	500	30	1000	3000	0.05	20000
Liver_Ramachandran	600	20	1000	7000	0.15	60000
Intestine_Martin	500	30	1000	6000	0.2	50000
CBDcs_He	800	10	1000	6500	0.15	50000
PBMC_He	1500	20	1000	7000	0.18	60000
Lung_He	600	10	800	7000	0.15	75000
Colon_He	600	10	800	7000	0.15	75000
Melanoma_He	600	10	800	6500	0.15	50000
Parameters for integrated DC dataset	500	10	1000	6000	0.15	50000

Table 4. List of top 50 DE genes in treated tumor cDCs

	cDC1_medium_vs_ IFNγ + TL8-506		cDC1_medium_vs_ Poly(I:C) + TL8-506		cDC1_IFNγ + TL8- 506_vs_Poly(I:C) + TL8- 506		cDC2_medium_vs_ IFNγ + TL8-506		cDC2_medium_vs_ Poly(I:C) + TL8-506		cDC2_IFNγ + TL8- 506_vs_Poly(I:C) + TL8- 506	
	gene	log2FC	gene	log2FC	gene	log2FC	gene	log2FC	gene	log2FC	gene	log2FC
1	IL12B	8.8	ITGB8	30.9	ISG15	3.3	IL12B	6.5	IL6	8.1	SIGLEC6	25.9
2	UBD	6.9	NCF2	30.2	OASL	3.0	IL6	6.3	TCF7L2	5.2	EVA1C	25.4
3	CCL3L1	6.2	WNT4	29.2	PEL1	2.8	CXCL9	5.5	STEAP1B	5.1	DKK1	25.2
4	CCL5	5.6	CCL3L1	8.8	CLCF1	2.2	CXCL10	5.5	CCL4	5.0	FAM9C	25.1
5	LTA	5.3	CCL4L2	7.8	PMAP1	1.7	UBD	5.4	TNF	5.0	FSTL1	25.1
6	CXCL9	4.9	CCL4	6.7	PSMB8	-1.5	IL36G	5.2	CCL4L2	4.8	IFNL1	25.1
7	GBP5	4.9	CCL3	6.6	CDC42SE2	-1.5	TNF	5.2	LTA	4.7	DAGLA	25.0
8	ITGB8	4.8	G0S2	6.0	WARS1	-1.6	ACOD1	5.1	CCL3L1	4.4	BIK	25.0
9	CCL3	4.8	NIP1	5.9	CD48	-1.7	LTA	5.0	HERC5	4.4	CCDC68	24.8
10	TCF7L2	4.6	TCF7L2	5.8	STAT1	-1.9	IL27	4.7	CD200	4.4	EFNA4	24.8
11	TNF	4.5	TNF	5.0	PCYT1A	-1.9	CXCL11	4.7	IGSF3	4.2	RANBP3L	24.7
12	PRR5L	4.5	EXT1	5.0	TAP1	-1.9	XIRP1	4.6	FXD6	4.0	ITGB5	24.7
13	IL1B	4.5	KMO	4.4	RIK3	-1.9	STEAP1B	4.6	CD40	4.0	MRPL38	24.7
14	SOCS2	4.5	OASL	4.1	CD274	-1.9	IL12A	4.3	TNFSF9	3.8	GRIN1	24.7
15	TBX21	4.4	TFRC	4.0	APOL2	-2.0	KREMEN1	4.2	DHX58	3.8	TPX2	24.6
16	CXCL10	4.4	PMAP1	3.9	HM13	-2.1	KCNJ2	4.1	IL23A	3.8	MEX3B	24.6
17	IGSF3	4.4	B3GNT7	3.6	STAT3	-2.1	IL1B	4.0	HLA-DOB	3.7	PIGR	24.6
18	IL27	4.2	FSD1L	3.5	LMNB1	-2.2	GBP5	4.0	CCL3	3.7	CCN2	24.6
19	CXCL11	4.1	GNS	3.5	RIPK2	-2.2	CCL4	3.8	SOCS1	3.6	MYOM1	24.5
20	G0S2	4.0	CLCF1	3.5	ITPR1P2	-2.3	CCL3	3.7	CKB	3.6	PORCN	24.5
21	SLC1A2	4.0	SOD2	3.5	CLIP1	-2.3	PDGFRA	3.7	CSRP2	3.5	FOXO2	24.5
22	ANKRD22	3.8	CXCL8	3.3	CD226	-2.4	CCL5	3.6	CCL5	3.5	ENOX1	24.5
23	FSD1L	3.8	SOCS3	3.0	PSMB9	-2.5	APOL4	3.6	G0S2	3.5	BICD1	24.5
24	CCL4L2	3.8	CDH1	2.9	LAP3	-2.6	GBP1	3.5	FSD1L	3.3	WDR27	24.5
25	BATF	3.7	MACROH2A2	2.9	IRF1	-2.8	ADIRF	3.5	IFNL1	3.1	NRG2	24.4
26	IL23A	3.5	PLAUR	2.9	UBE2L6	-2.9	TBX21	3.3	IL1B	3.1	FABP3	24.4
27	GBP1	3.4	STAT5A	2.8	CXCL11	-2.9	GPR171	3.3	RAB3IP	3.0	GATD3B	24.3
28	ELOVL7	3.4	SLC7A1	2.6	TRAFD1	-3.1	CCL3L1	3.2	CLCF1	2.9	FANCD2	24.3
29	TNFAIP6	3.3	HLA-DOB	2.6	CSF2RB	-3.1	JAG1	3.2	RIPOR2	2.9	ARHGEF19	24.3
30	ETV7	3.3	CCR7	2.6	GBP2	-3.1	CSF3	3.2	ATP6V0A2	2.9	ANKS6	24.3
31	MYC	3.2	NOP58	2.6	MSRB1	-3.7	G0S2	3.2	EXT1	2.9	TMSB15A	24.2
32	EXT1	3.2	NHP2	2.5	GBP5	-3.8	IGSF3	3.2	ITGA1	2.9	FANCB	24.2
33	RAB33A	3.2	CD44	2.4	CXCL10	-4.4	SOCS1	3.2	PIM1	2.8	ESPL1	24.2
34	GBP4	3.1	B4GALT5	2.4	GBP4	-4.4	IL2RA	3.1	NFKBIZ	2.8	CMTM4	24.2
35	CCND2	3.1	INSIG1	2.4	CXCL9	-5.4	CD274	3.1	TMEM268	2.7	PLOD2	24.2
36	CCL4	3.1	NFKBIZ	2.4	HAPLN3	-5.8	FJX1	3.1	EB3	2.7	EFCAB11	24.1
37	CD274	3.1	UTP6	2.4	GBP1	-6.8	NFKBIZ	3.0	GALNT3	2.6	FRAT1	24.1
38	SOCS1	3.0	FOXP1	2.4			HECW2	3.0	PMAP1	2.6	LAMC2	24.1
39	SOCS3	3.0	THAP2	2.3			LIMK2	3.0	FAM126A	2.6	ST6GALNAC2	24.1
40	CREB5	2.9	CD40	2.3			FXD6	2.9	TUBB2A	2.6	CCDC24	24.1
41	NFKBIZ	2.9	DDX21	2.3			HLA-DOB	2.9	IF44	2.6	TONSL	24.1
42	CSF2RB	2.8	MAP3K8	2.2			ETV7	2.9	RAB29	2.6	EYA2	24.1
43	SOD2	2.8	PEL1	2.1			SOCS3	2.9	NEDD4L	2.5	LRRC26	24.1
44	TCFL5	2.8	NANS	2.1			IL1A	2.8	SOCS3	2.5	IFT81	24.0
45	IL15	2.8	GTPBP4	2.0			IDO1	2.7	HERC6	2.5	ZSCAN20	24.0
46	PRDM1	2.6	ISG20	1.9			CCL4L2	2.7	OASL	2.5	NLRP2	24.0
47	IL1A	2.6	CDK6	1.9			FSD1L	2.7	FLT1	2.5	TBC1D3L	24.0
48	HAPLN3	2.6	WTAP	1.8			GBP4	2.7	TAGAP	2.5	IL22RA2	24.0
49	CDH1	2.6	MGLL	1.8			CD40	2.6	KIF3B	2.5	DNAH10	24.0
50	KMO	2.6	IL2RA	1.8			PDCD1LG2	2.6	STK17B	2.5	H3C4	24.0

	aDC_tumor in situ_vs_ IFN γ + TL8-506 ex vivo		aDC_tumor in situ_vs_ Poly(I:C) + TL8-506 ex vivo		aDC+intcDC2_tumor in situ_vs_ IFN γ + TL8-506 ex vivo		aDC+intcDC2_tumor in situ_vs_ Poly(I:C) + TL8-506 ex vivo	
	gene	log2FC	gene	log2FC	gene	log2FC	gene	log2FC
1	LTA	29.4	WNT4	6.7	LTA	29.5	LTA	29.2
2	TBKBP1	6.1	ZBTB32	6.3	CCL3	6.9	IFNB1	8.8
3	CXCL10	5.6	TNF	6.0	TNF	6.0	CSF2	7.8
4	TNF	5.4	CCL3	5.2	IL1B	5.9	IL12A	7.2
5	WNT4	5.4	IL1B	4.7	IL12A	5.8	CCL3	6.9
6	GBP5	5.3	IL6	4.7	CCL4	5.7	WNT4	6.7
7	CXCL11	5.2	CCL4	4.7	CXCL10	5.7	CCL4	6.6
8	TCF7L2	5.0	LAMC1	4.7	CSF2	5.6	TNF	6.4
9	IL27	4.8	TCF7L2	4.6	GBP5	5.3	IL1B	6.2
10	CXCL9	4.8	RASSF8	4.5	CXCL11	5.3	IL6	6.0
11	IL1B	4.7	EXT1	4.3	KCNJ2	5.2	STEAP1B	5.9
12	CCL3	4.5	NIP1	4.3	IL27	5.1	IL1A	5.8
13	AIM2	4.5	ABAT	4.3	WNT4	5.1	EPB41L5	5.6
14	SNTB1	4.4	GALNT12	4.3	SERPINB2	5.0	ZBTB32	5.4
15	IL6	4.3	TCFL5	4.3	IL6	4.9	CCL5	4.9
16	P2RY6	4.2	IL1R1	4.3	TBKBP1	4.9	RASSF8	4.9
17	SLAMF8	4.2	B3GNT7	4.2	IL1A	4.7	TLCD1	4.8
18	TCFL5	4.2	APOBR	4.1	STEAP1B	4.7	B3GNT7	4.8
19	TLR4	4.1	TLCD1	4.0	CXCL9	4.7	OASL	4.7
20	GBP7	4.1	MGST1	4.0	MEFV	4.6	EXT1	4.7
21	IL12B	4.0	HERC5	3.9	PLEKHN1	4.5	IL1R1	4.6
22	PRR5L	3.9	IGSF3	3.8	CSF3	4.4	BAALC	4.6
23	CDH1	3.9	TACSTD2	3.7	CCL5	4.4	NIP1	4.6
24	GBP4	3.8	CCL5	3.6	GBP1	4.4	ITGA1	4.5
25	GBP1	3.8	IL2RA	3.6	TCF7L2	4.3	IGSF3	4.5
26	TBX21	3.8	SGMS2	3.6	CACNA1A	4.3	LAMC1	4.4
27	APOBR	3.8	NFKBIZ	3.5	BAALC	4.2	HERC6	4.4
28	IGSF3	3.8	PDGFB	3.4	RAB33A	4.2	TJP1	4.4
29	CMPK2	3.7	IL12B	3.4	AQP9	4.2	IL23A	4.3
30	RAB33A	3.7	PLAUR	3.4	DNAF1	4.2	AMIGO2	4.2
31	POU3F1	3.6	MBP	3.4	P2RX7	4.2	GALNT12	4.2
32	TLCD1	3.6	GALNT3	3.3	EPB41L5	4.1	HERC5	4.2
33	DLL4	3.6	GRWD1	3.3	CMPK2	4.1	TCF7L2	4.2
34	CCL5	3.6	NEDD4L	3.3	CD300E	4.1	SHROOM1	4.2
35	SMN1	3.6	TCF7	3.2	TLR4	4.1	IL2RA	4.2
36	ZBTB6	3.5	G0S2	3.2	GBP7	4.1	NEDD4L	4.1
37	EXT1	3.4	ZMYND11	3.1	ATP10A	4.1	CLCF1	4.0
38	PAWR	3.4	MAP4K5	3.1	INHBA	4.0	CDH1	3.9
39	CASP10	3.4	CLCF1	3.1	PRR5L	3.9	KIAA1522	3.9
40	NFKBIZ	3.4	CD40	3.1	KCNN4	3.9	IL1RN	3.8
41	SCARF1	3.3	PMAIP1	3.1	EXT1	3.8	IFT2	3.8
42	IRF8	3.3	IGF2R	3.1	DYRK3	3.8	TRAF3IP2	3.8
43	ZFYVE28	3.3	HAUS6	3.1	TBX21	3.8	TCFL5	3.8
44	ETV7	3.3	RFFL	3.1	NEU4	3.7	IL12B	3.8
45	CCL4	3.2	FOSL1	3.1	OASL	3.7	LIMS2	3.8
46	EPC2	3.2	MFHAS1	3.0	ITGA1	3.7	MACC1	3.7
47	IL2RA	3.2	PLAGL2	3.0	AIM2	3.6	SNTB1	3.7
48	GPATCH4	3.2	FAM126A	3.0	ZFYVE28	3.6	GALNT3	3.7
49	APOL1	3.2	PRKCI	3.0	IGSF3	3.6	DDX60	3.7
50	DYRK3	3.1	CDC42EP3	3.0	GBP4	3.6	G0S2	3.7

Table 5. Overview of patient tumor samples

sample_ID	Tumor Indication	Subtype	Patient Treatment	Assays	% CD45 ⁺ cells	Panel for flow cytometry
colon_1	Colon cancer	liver metastasis	untreated	scRNA-seq, flow cytometry	30	FACSAria III , FACSsymphony A5
lung_1	Lung cancer	Adeno carcinoma	untreated	scRNA-seq	75	FACSAria III
lung_2	Lung cancer	NSCLC	untreated	flow cytometry, ELISA	44	LSRFortessa
lung_3	Lung cancer	NSCLC	untreated	flow cytometry	72	LSRFortessa
lung_4	Lung cancer	NSCLC	untreated	flow cytometry	74	LSRFortessa
melanoma_1	Melanoma	lymph node metastasis	untreated	scRNA-seq	96	FACSAria III
melanoma_2	Melanoma	lymph node metastasis	untreated	scRNA-seq, flow cytometry	15	FACSAria III, FACSsymphony A5
melanoma_3	Melanoma	lymph node metastasis	untreated	flow cytometry	98	FACSsymphony A5
melanoma_4	Melanoma	lymph node metastasis	untreated	flow cytometry	15	LSRFortessa
melanoma_5	Melanoma	brain metastasis	LGX818+MEK162, lpi+Nivo, Nivo	flow cytometry	21	LSRFortessa
melanoma_6	Melanoma	lymph node metastasis	untreated	flow cytometry	18	LSRFortessa
ovarian_1	Ovarian cancer	serous carcinoma	untreated	ELISA	61	-
ovarian_2	Ovarian cancer	serous carcinoma	untreated	ELISA	59	-

Materials and Methods

ScRNA-seq data quality control and pre-processing

Publicly available scRNA-seq datasets of different tissues (online supplemental table 2) were collected either as raw count matrices or fastq files. Internal and external fastq files were aligned and quantified using the Cell Ranger Single-Cell Software [1] with default parameters against the GRCh38 human reference genome. The data was further pre-processed by following the standard workflow in Besca [2]. For individual datasets, the quality of cells was assured by filtering all low-quality cells and removing uninformative genes by using the parameters in online supplemental table 3. The filtering was applied to cells based on the metrics, including minimum and maximum number of genes expressed, minimum and maximum total UMI count, and maximum proportion of mitochondrial gene count. Also, genes that were expressed in less than 10 cells were filtered out. After performing quality control, the raw count data were normalized, logarithmized and used for several downstream studies.

Dimension reduction and unsupervised clustering

For each dataset, the genes showing highest variability using `besca.st.highly_variable_genes` function were selected (minimal mean = 0.0125, maximal mean = 3 and minimal normalized dispersion = 0.5 cutoffs). Next, the effects of total count per cell and mitochondrial gene percentage effects were regressed out and the data were standardized. Subsequently, a principal component analysis with 50 components was performed and the first 50 components retained to build a nearest neighbor graph (local neighborhood size 15) and to derive clusters using the Leiden community detection

algorithm [3]. To integrate the cells from public datasets into a shared space, the raw datasets were concatenated and a second round of preprocessing, quality control was performed. The calculated PCA matrix was subjected to the Harmony algorithm [4] as an input, and individual studies were kept as a technical covariate for the correction. The batch-corrected PCA coordinates were then used to build the integrated nearest neighbor graph and to find clusters within. For the visualization of identified clusters, the Harmony corrected PCA matrix as an input was used for the UMAP. Further, Gaussian kernel density estimation function from scanpy was used to calculate the density of tumor-derived treated and non-treated immune cells, as well as tumor-derived cells from public datasets in the UMAP space [5].

Cell type annotation

To identify the cell type of the clusters returned by the Leiden algorithm, curated signatures and the sig-annot workflow available in Besca were used [2] based on the expression of signature markers. After identifying major cell types in the pooled dataset, myeloid dendritic cells were separated and the third round of pre-processing and cell-type annotation was performed to explore subpopulations with higher resolution. The third round is similar to the second round of pre-processing, where the raw and unfiltered gene expression concatenated matrix of only the identified myeloid dendritic cells was used and filtering (parameters in online supplemental table 3), HVG identification, PCA computation, and batch correction by Harmony algorithm was performed.

Differential expression analysis

Differential expression (DE) analysis between different cell groups was performed using a Wilcoxon Rank Sum test and multiple hypothesis testing correction using the Benjamini-

Hochberg procedure (function `scanpy.tl.rank_genes_groups`). To avoid the possible bias resulting from the comparison of imbalanced cell groups, when needed, each cell group was downsampled to the minimum number of all cell groups. The adjusted p-value threshold was kept at 0.05 and genes with less than this value were considered as significantly differentially expressed. Top DE genes were selected based on the highest log₂ fold change (log₂FC). Top 50 DE genes are listed in online supplemental table 4.

Velocity analysis

The Velocity 0.17.17 package [6] was used to obtain spliced and unspliced read counts from the previously aligned scRNA-seq files from melanoma, lung and colon cancer samples and RNA velocity was calculated using the scvelo 0.2.3 package [7]. To keep the embedding consistent with the integrated dataset, the batch corrected PCA space was used to calculate the nearest neighbor graph. For each cell, the RNA velocity of genes was used to generate the RNA velocity vector embedding. For this, the first and second-order moments among nearest neighbor cells in reduced PCA space were computed. Further, the data and calculated moments were subjected to the RNA velocity estimation by modeling the full transcriptional dynamics of splicing kinetics (dynamical model).

CD8⁺ T cell migration assay

Observation windows were filled with 50 μ L cold PBS. Collagen mixture (4 mg/mL rat collagen, R&D, #3440-100-01, in 0.1 M HEPES, Life Technologies, #15630-122, 3.7 g/L NaHCO₃, Lonza, #BE17-613E) was prepared on ice and 2 μ L was pipetted into the middle channel of a cold 3-lane OrganoPlate (MIMETAS, #4004-400-B) to build the extracellular matrix barrier. After 30 min of polymerization at 37°C, 30 μ L PBS were added to the inlet

of the collagen channel to prevent collagen drying. OrganoPlate was left overnight in the cell culture incubator. The next day, PBS was removed from the collagen inlets, 2×10^4 human umbilical vein endothelial cells (HUVECs, Lonza, #C2517AS) were seeded in $2 \mu\text{L}$ HUVEC medium (EGM-2, Lonza, #CC-3162/6) into the inlet of the top channel. $50 \mu\text{L}$ HUVEC medium was added to the inlet of the top channel. HUVECs were allowed to attach to the collagen interface for 2 hours in the cell culture incubator. $50 \mu\text{L}$ HUVEC medium was then added to the outlet of the top channel. After 6 days of HUVEC vessel formation at 37°C in a CO_2 incubator, HUVEC medium was removed from the inlets and outlets of the top channel. 2×10^5 activated CD8^+ T cells in $100 \mu\text{L}$ T cell medium (RPMI, Gibco, #42401-018, 10% FBS, 1% Pen/Strep, 1% Sodium Pyruvate, 1% Non-Essential Amino Acids Solution, Gibco, #11140-050, 1% GlutaMAX, Gibco, #35050-061, $50 \mu\text{M}$ 2-Mercaptoethanol, Gibco, #31350-010) were plated into the top channel. CD8^+ T cells were isolated from PBMCs using the Miltenyi CD8^+ T Cell Isolation Kit (#130-096-495) and activated for 4 days using CD3/CD28 activator (STEMCELL, #10971) according to the manufacturer's protocol. CD8^+ T cells were labeled with 1 mM CFMFA (Life Technologies, #C7025) for 15 min at 37°C right before plating into the OrganoPlate. Supernatants of stimulated cord blood cDCs, 1:1 diluted in T cell medium were added to the bottom channel. T cell migration was measured in the collagen layer after 48 hours at 37°C in a CO_2 incubator using the PerkinElmer Operetta High Content Imaging System. After 72 hours of migration, cells in the collagen layer were fixed using 0.4% formaldehyde (Sigma, #47608) in PBS for 15 min at room temperature. Cells were washed 2x with PBS and permeabilized using 0.3% Triton X-100 (Sigma, #T8787) for 10 min at room temperature. The plate was washed 1x with 4% FBS in PBS and blocked with 2% FBS, 2% BSA, 0.1% Tween20 (Sigma, #P2287) in PBS for 30 min at room temperature. Cells were stained

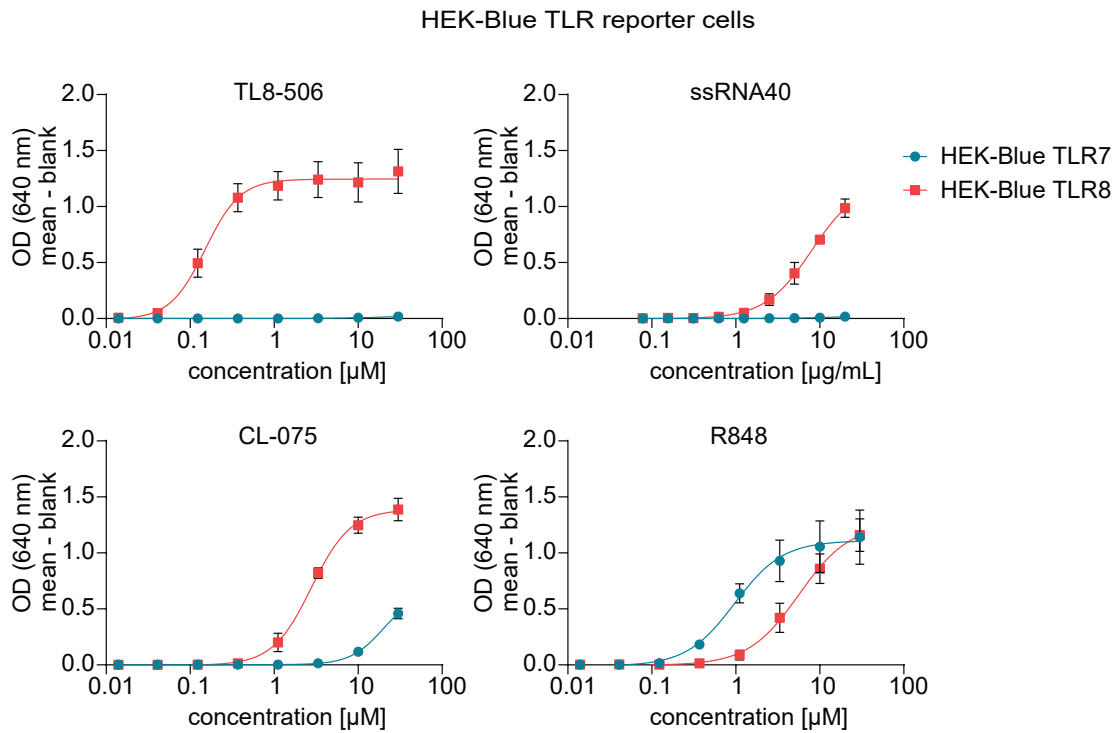
with anti-CD8 antibodies (BD, #555635) in 2% FBS, 2% BSA, 0.1% Tween20 in PBS for 4 hours at room temperature. The plate was washed 2x with 4% FBS in PBS, 1x with PBS. Stained cells were detected using the PerkinElmer Operetta High Content Imaging System. Quantification of the migrated T cells was done using ImageJ.

References

1. Zheng, G.X.Y., et al., *Massively parallel digital transcriptional profiling of single cells*. Nature Communications, 2017. **8**.
2. Madler, S.C., et al., *Besca, a single-cell transcriptomics analysis toolkit to accelerate translational research*. NAR Genom Bioinform, 2021. **3**(4): p. lqab102.
3. Traag, V.A., L. Waltman, and N.J. van Eck, *From Louvain to Leiden: guaranteeing well-connected communities*. Scientific Reports, 2019. **9**.
4. Korsunsky, I., et al., *Fast, sensitive and accurate integration of single-cell data with Harmony*. Nat Methods, 2019. **16**(12): p. 1289-1296.
5. Wolf, F.A., P. Angerer, and F.J. Theis, *SCANPY: large-scale single-cell gene expression data analysis*. Genome Biology, 2018. **19**.
6. La Manno, G., et al., *RNA velocity of single cells*. Nature, 2018. **560**(7719): p. 494-498.
7. Bergen, V., et al., *Generalizing RNA velocity to transient cell states through dynamical modeling*. Nature Biotechnology, 2020. **38**(12).

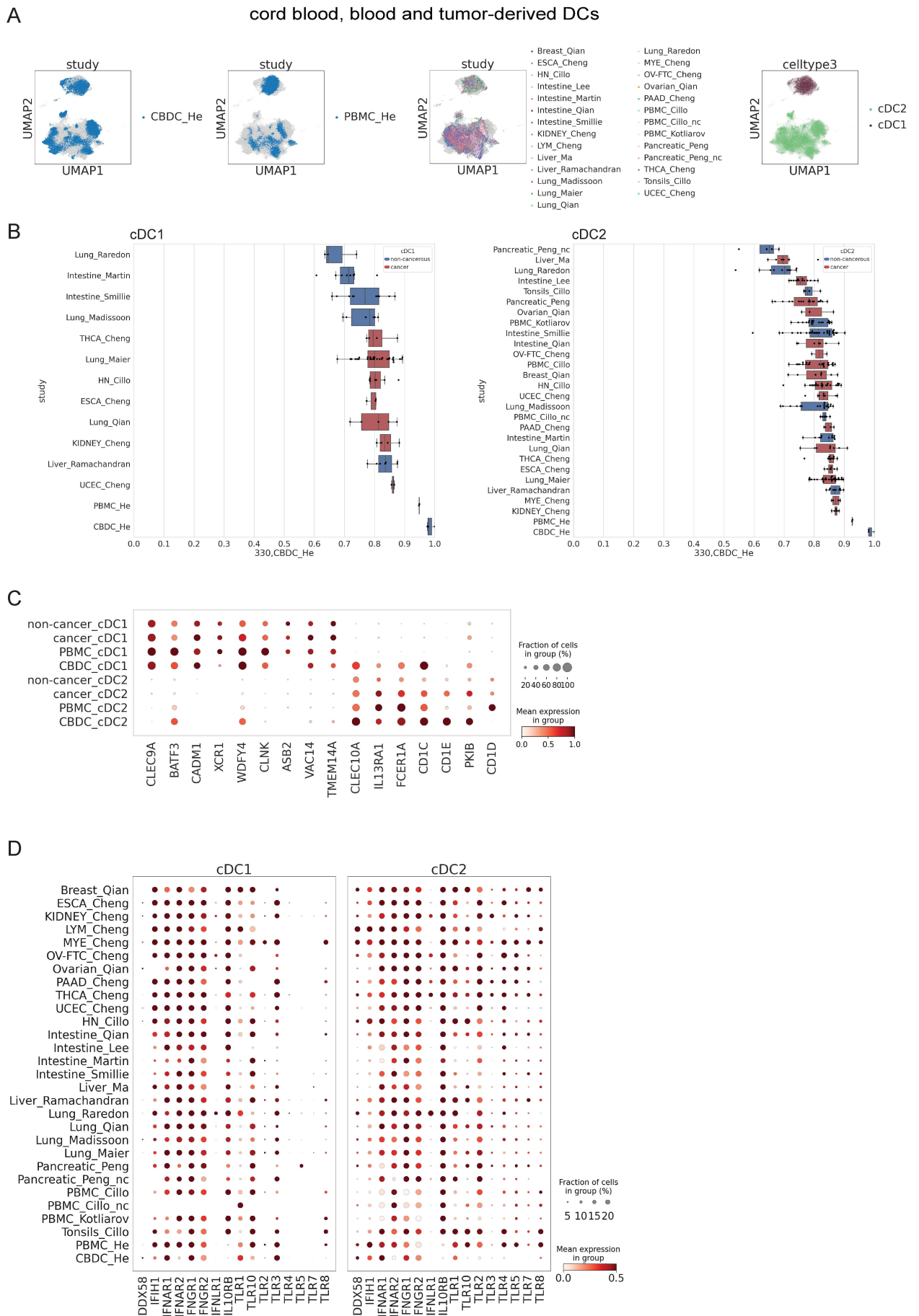
Supplementary Figures

Figure S1



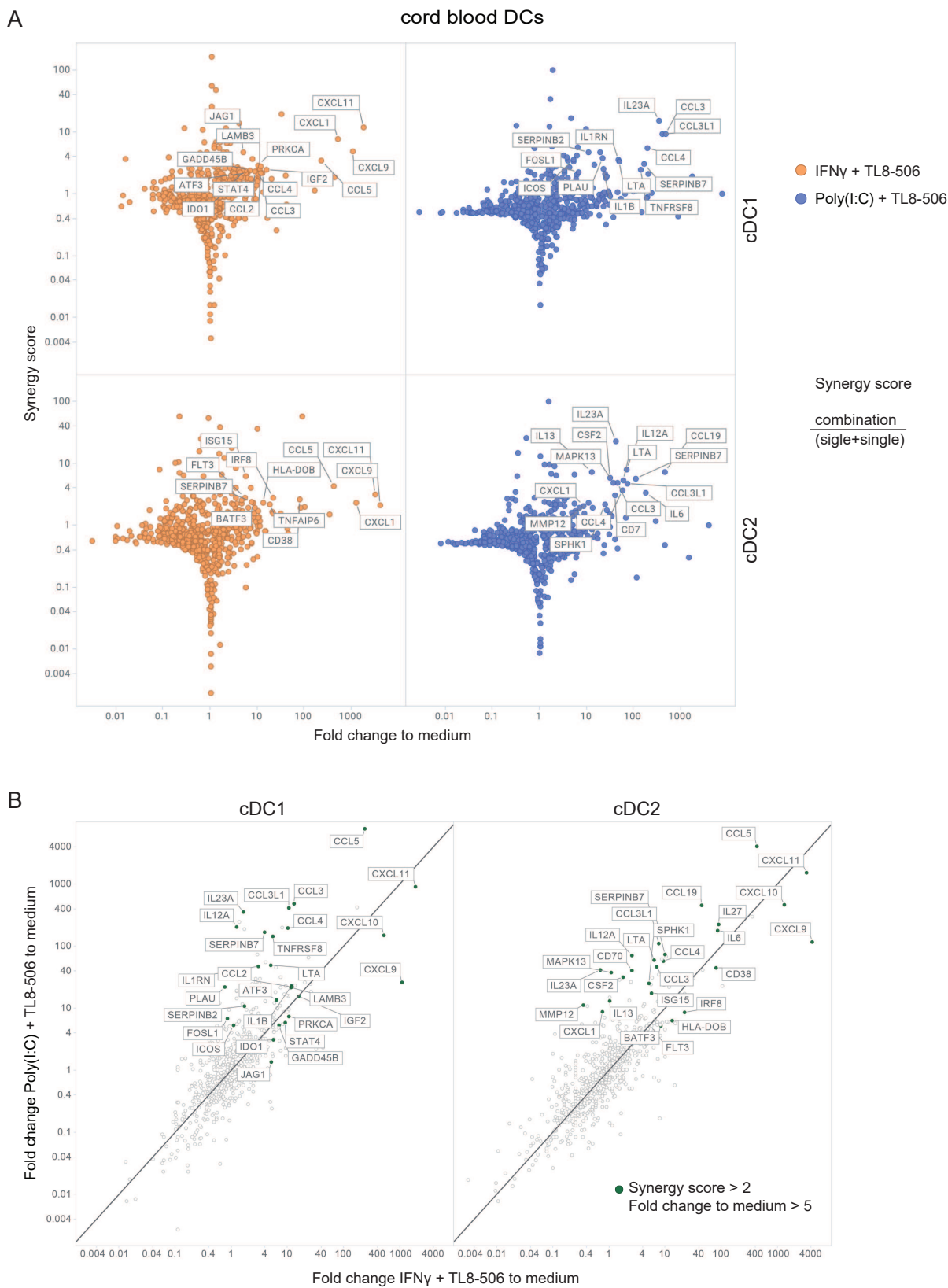
Supp. Figure 1 TL8-506 is selective for human TLR8 and does not activate human TLR7. HEK-Blue cells that were engineered to express the human TLR7 or TLR8 and the NF- κ B-inducible SEAP (secreted embryonic alkaline phosphatase) reporter gene were treated with the indicated agonists and concentrations for 18 hours. Real-time detection of SEAP activity by performing the colorimetric enzyme assay in HEK-Blue Detection medium, from three independent experiments, mean+SEM is shown.

Figure S2



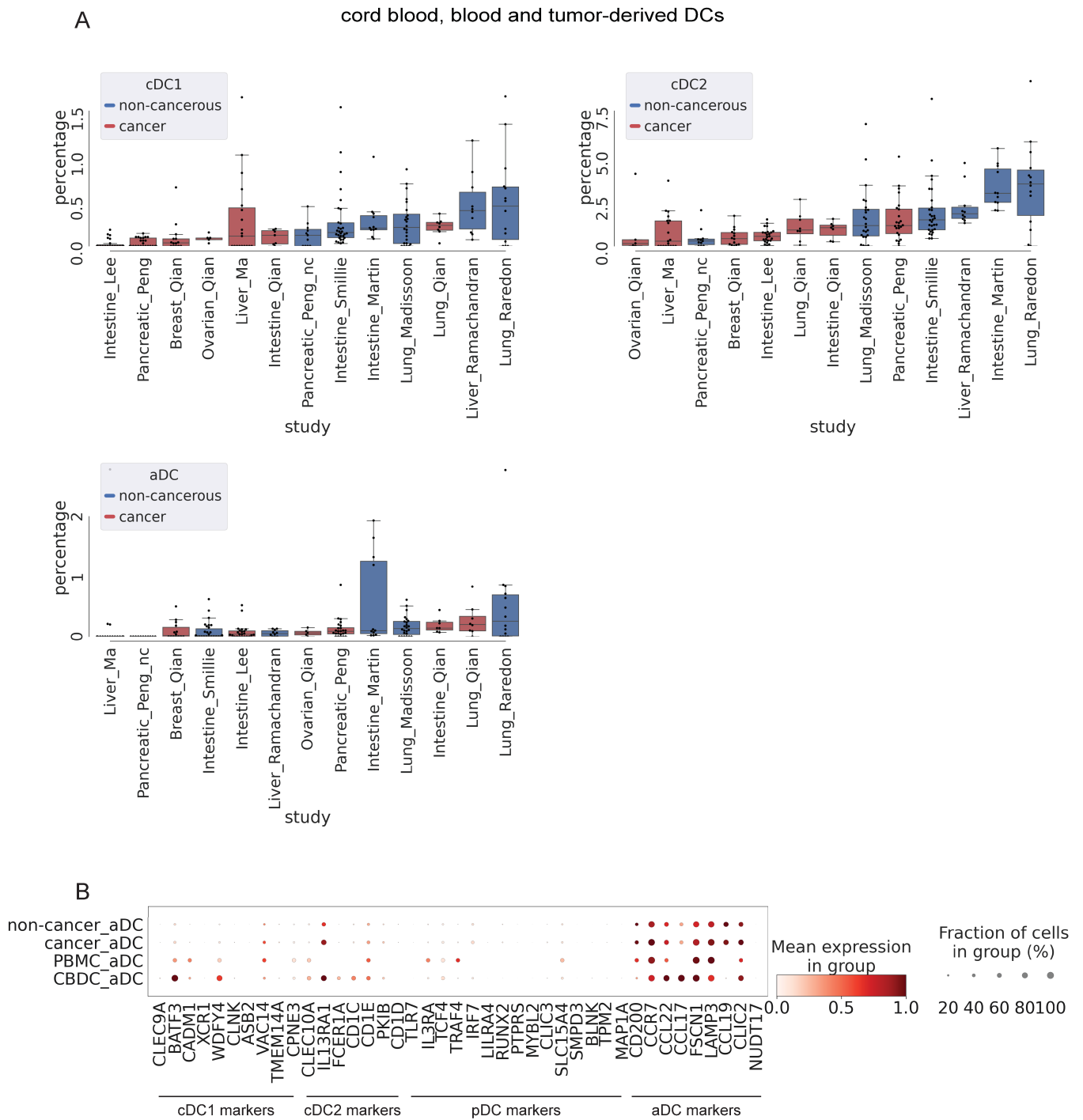
Supp. Figure 2 Human cord blood, blood and tumor cDCs show comparable gene expression. 10x Genomics scRNA-seq was performed on FACS sorted blood cDCs (PBMC), n=2 donors, from one experiment, and in vitro differentiated cord blood cDCs (CBDC) harvested on day 12, n=3 batches of cord blood from mixed donors, 6 donors in total, from two independent experiments. scRNA-seq data of tissue cDCs (non-cancer and cancer) were integrated from different public studies listed in online supplemental table 2. (A) UMAP of 59'025 cDCs profiled across different scRNA-seq studies with each cell color-coded for study or cDC subset. (B) Spearman correlation values are shown comparing cord blood cDCs with blood and tissue cDCs. Correlation values were calculated based on the mean expression of genes per cell subset and donor. (C) Fraction positive and mean expression of different cDC subset-specific markers in cord blood, blood and tissue cDC1s or cDC2s. Mean expression was calculated across all the cells in the group and then scaled to a 0-1 range. (D) Fraction positive and mean expression of different IFNRs and PRRs in cord blood, blood and tissue cDC1s or cDC2s. Mean expression was calculated across all the cells in the group and then scaled to a 0-1 range.

Figure S3



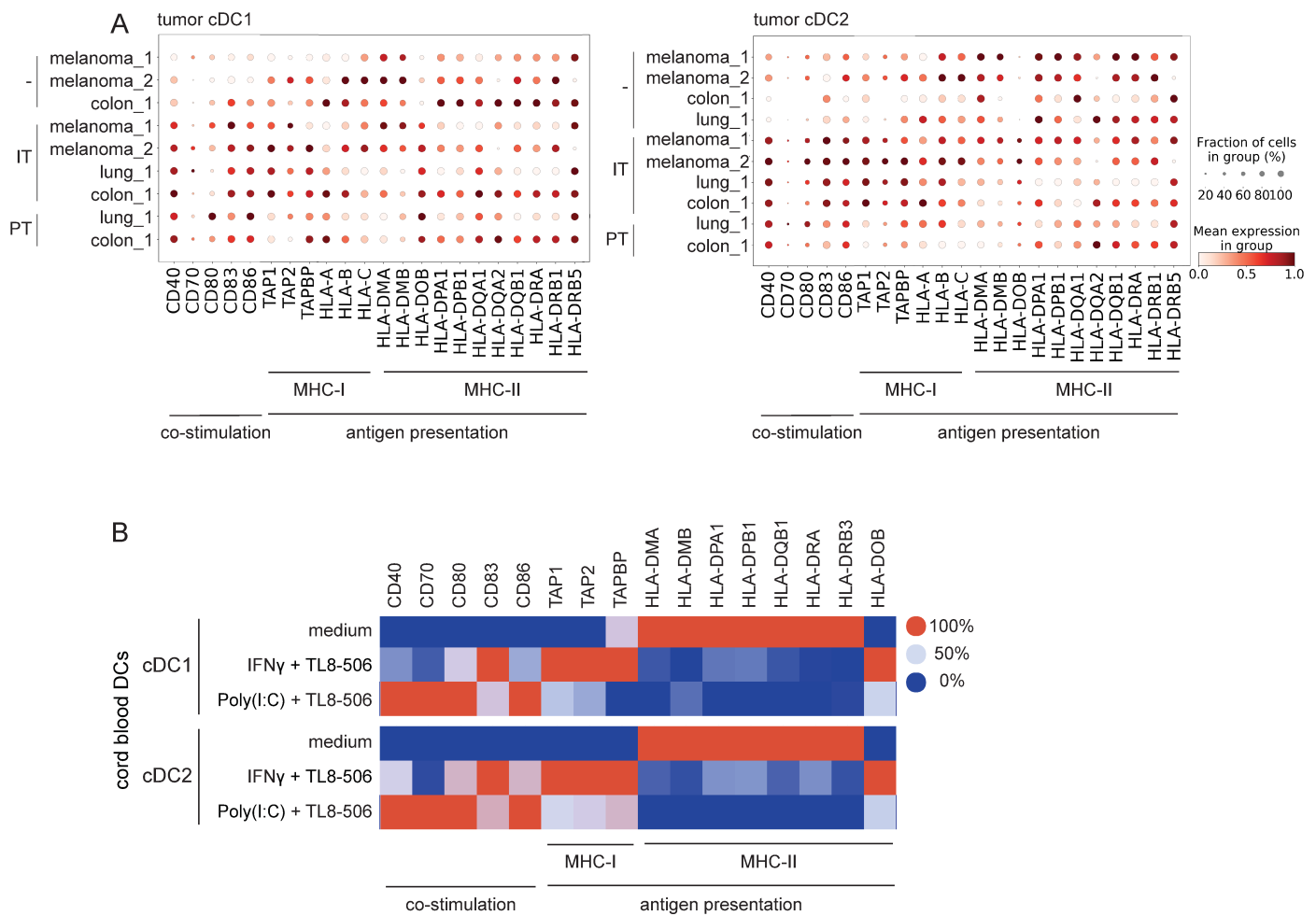
Supp. Figure 3 IFN γ + TL8-506 or Poly(I:C) + TL8-506 synergize to upregulate different genes in cord blood cDCs. Cord blood cDCs were sorted by FACS and stimulated with the indicated stimuli for 15 hours. Gene expression was analyzed in cell lysates using the NanoString human Myeloid Innate Immunity panel, n=2 batches of cord blood from mixed donors, in total 4 donors, from two independent experiments, representative data are shown for 1 batch of cord blood from mixed donors (2 donors). (A) For each gene, synergy scores for combinatorial stimulation is plotted against fold change in expression in stimulated cDCs, calculation of synergy score for each gene is depicted on the right, labeled genes have a synergy score >2 and fold change to medium >5. (B) For each gene, fold change in expression in IFN γ + TL8-506 treated cDCs is plotted against fold change in expression in Poly(I:C) + TL8-506 treated cDCs, comparing the genes highly induced by IFN γ + TL8-506 vs Poly(I:C) + TL8-506 treatment. Labeled genes have a synergy score >2 and fold change to medium >5. The following concentrations were used for DC stimulation: 50'000 U/mL huIFN γ , 10 μ g/mL Poly(I:C), 1 μ M TL8-506.

Figure S4



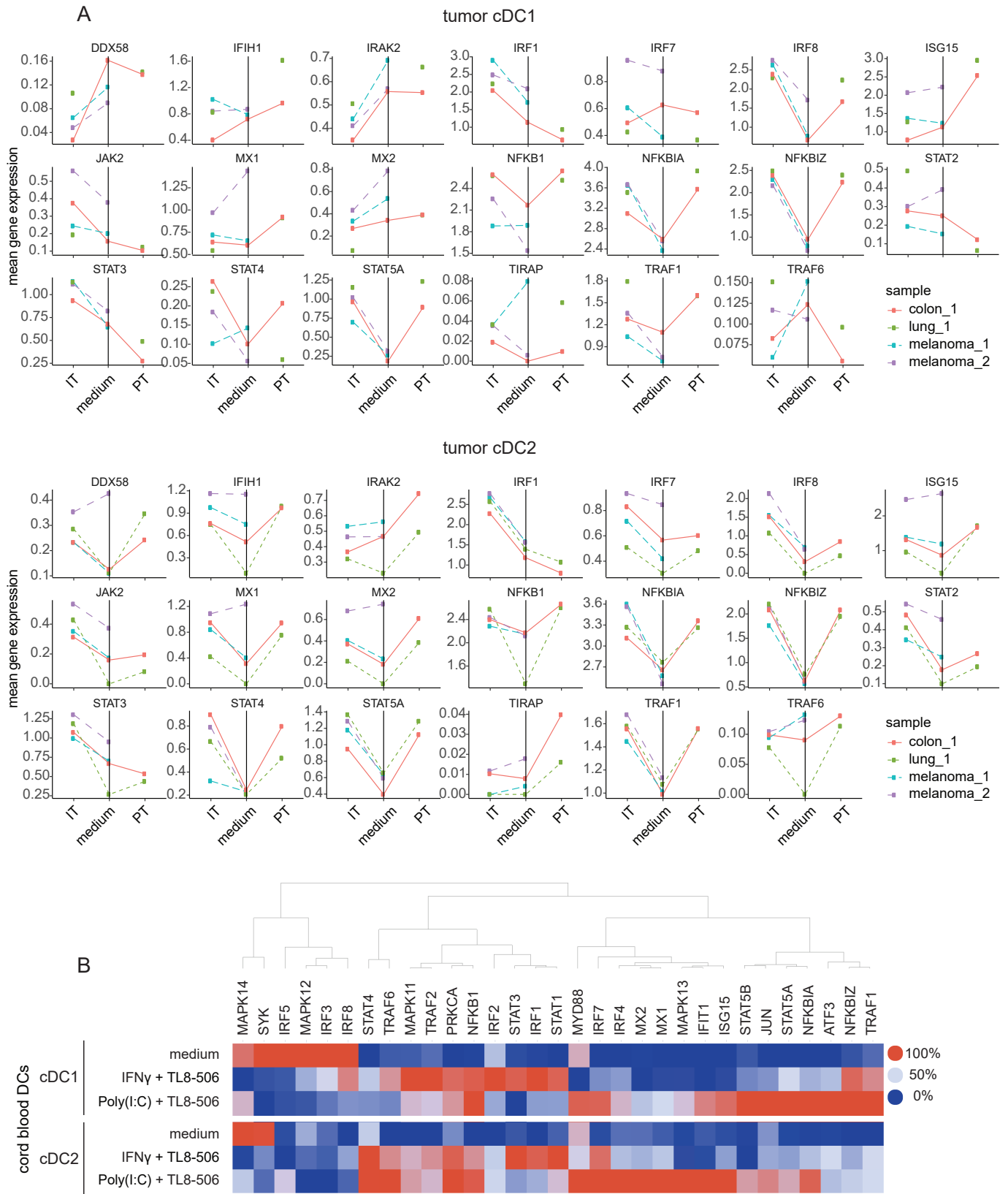
Supp. Figure 4 cDCs with an activated phenotype are rare across different human tumor indications. (A) Percentage of cDC1s, cDC2s and activated DCs (aDCs) of all cells (CD45⁺ and CD45⁻ cells) from the processed tissue samples was calculated and depicted. Only studies in which the entire tissue was proved by scRNA-seq without prior cell type enrichment were included. (B) DC subset-specific markers were analyzed in the activated DC (aDC) population from all scRNA-seq studies. Fraction positive and mean expression of DC subset-specific markers in aDCs from tissue (non-cancer, cancer), blood (PBMC) and cord blood (CBDC) is shown. Mean expression was calculated across all the cells in the group and then scaled to a 0-1 range.

Figure S5



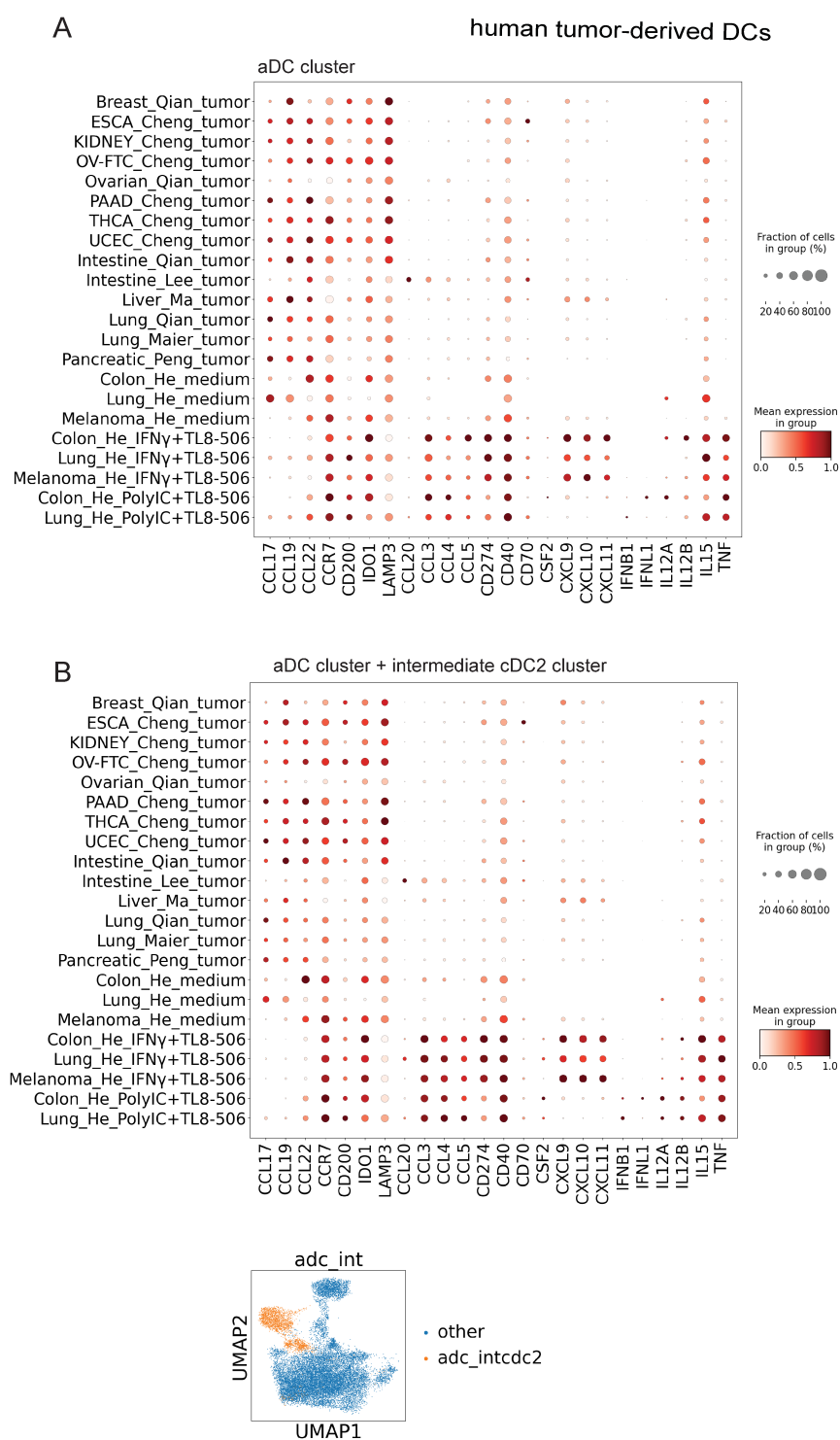
Supp. Figure 5 Tumor cDCs activated by TL8-506 combinations up-regulate genes involved in co-stimulation and antigen presentation. (A) Digested tumor samples from melanoma, CRC and lung cancer patients were treated with 1 μ M TL8-506 + 50'000 U/mL IFN γ or 1 μ M TL8-506 + 10 μ g/mL Poly(I:C) for 4 hours. 10x Genomics scRNA-seq was performed on FACS sorted CD45⁺, CD3⁻ cells, n=4 donors, from three independent experiments. Fraction positive and mean expression of co-stimulatory molecules and genes involved in antigen presentation in tumor-derived cDC1s and cDC2s upon treatment with TL8-506 combinations is shown. Mean expression was calculated across all the cells in the group and then scaled to a 0-1 range, - = medium, IT = IFN γ + TL8-506, PT = Poly(I:C) + TL8-506. (B) Cord blood cDCs were sorted by FACS and stimulated with 1 μ M TL8-506 + 50'000 U/mL IFN γ or 1 μ M TL8-506 + 10 μ g/mL Poly(I:C) for 15 hours. Gene expression was analyzed in cell lysates using the NanoString human Myeloid Innate Immunity panel, n=2 batches of cord blood from mixed donors, 4 donors in total, from two independent experiments, colors displaying the maximum (100%) to minimum (0%) mean gene expression per column.

Figure S6



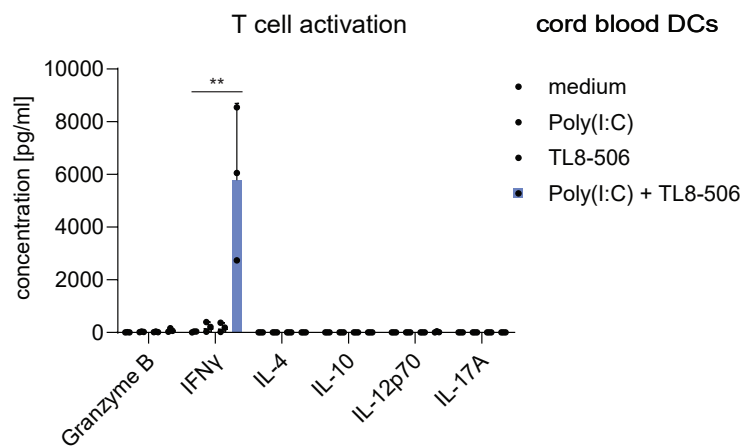
Supp. Figure 6 TL8-506 combinations induce TLR and IFN signaling in treated tumor cDCs. (A) Digested tumor samples from melanoma, CRC and lung cancer patients were treated with 1 μ M TL8-506 + 50'000 U/mL IFN γ or 1 μ M TL8-506 + 10 μ g/mL Poly(I:C) for 4 hours. 10x Genomics scRNA-seq was performed on FACS sorted CD45⁺, CD3⁻ cells, n=4 donors, from three independent experiments. Mean gene expression of components of the TLR and IFN pathways in tumor cDC1s and cDC2s is displayed, IT = IFN γ + TL8-506, PT = Poly(I:C) + TL8-506. (B) Cord blood cDCs were sorted by FACS and stimulated with 1 μ M TL8-506 + 50'000 U/mL IFN γ or 1 μ M TL8-506 + 10 μ g/mL Poly(I:C) for 15 hours. Gene expression was analyzed in cell lysates using the NanoString human Myeloid Innate Immunity panel, n=2 batches of cord blood from mixed donors, 4 donors in total, from two independent experiments, colors displaying the maximum (100%) to minimum (0%) mean gene expression per column.

Figure S7



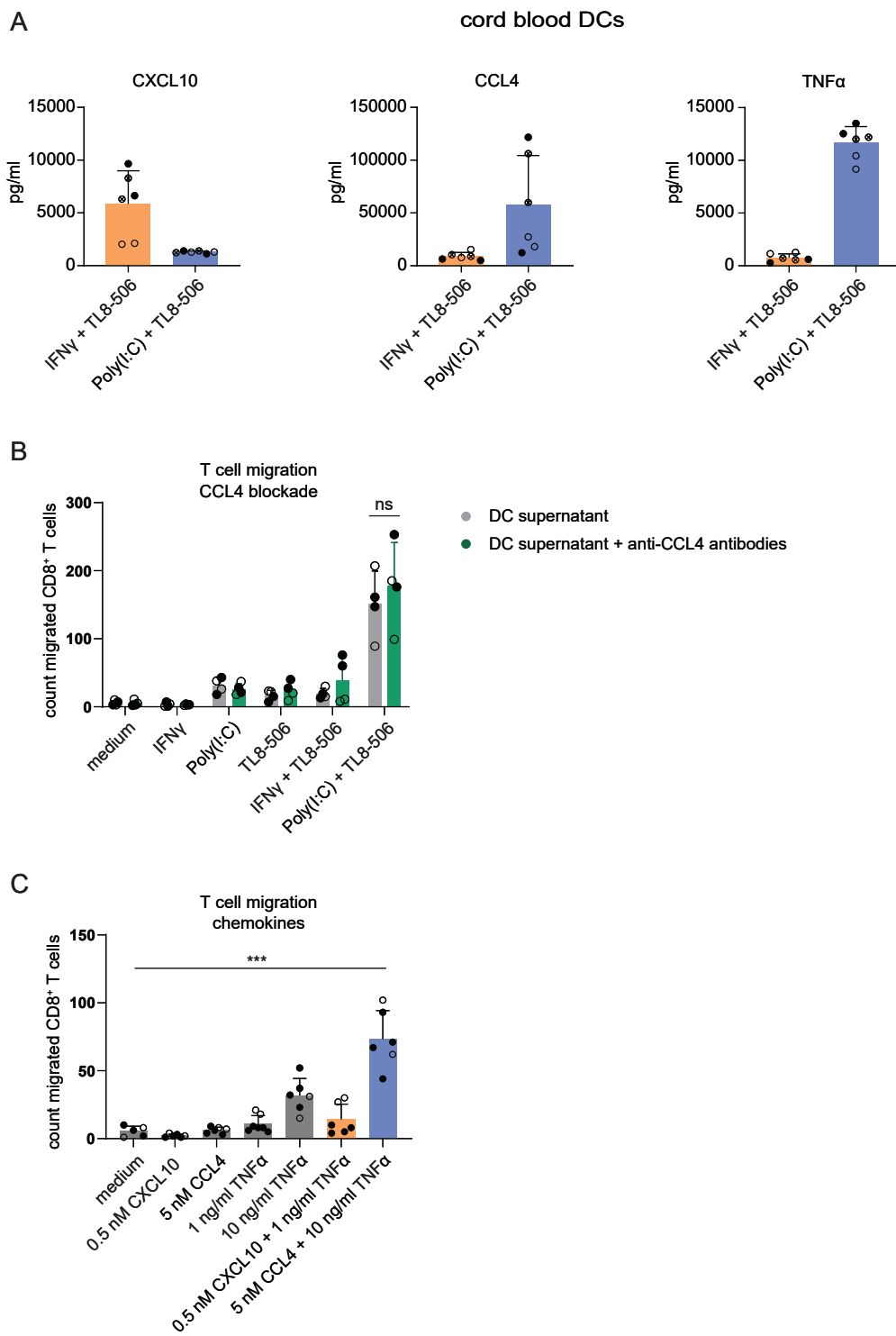
Supp. Figure 7 Tumor-derived cDCs activated by TL8-506 combinations show increased expression of activation markers compared to in situ activated cDCs from different human tumor indications. Digested patient tumor samples were treated with 1 μ M TL8-506 + 50'000 U/mL IFN γ or 1 μ M TL8-506 + 10 μ g/mL Poly(I:C) for 4 hours. scRNA-seq was performed on FACS sorted CD45⁺, CD3⁻ cells, n=4 donors, from three independent experiments. scRNA-seq data of in situ activated cDCs were integrated from different public studies listed in online supplemental table 2. (A) Fraction positive and mean expression of activation markers in activated DCs (aDCs), stratified per treatment, study and tissue of origin. Only cDCs falling into the aDC cluster were analyzed. Mean expression was calculated across all the cells in the group and then scaled to a 0-1 range. (B) Fraction positive and mean expression of activation markers in activated DCs (extended population), stratified per treatment, study and tissue of origin. Cells color-coded in orange from the aDC cluster and intermediate cluster between aDCs and cDC2s were analyzed, adc_intcdc2 = aDC cluster + intermediate cDC2 cluster. Mean expression was calculated across all the cells in group and then scaled to a 0-1 range.

Figure S8



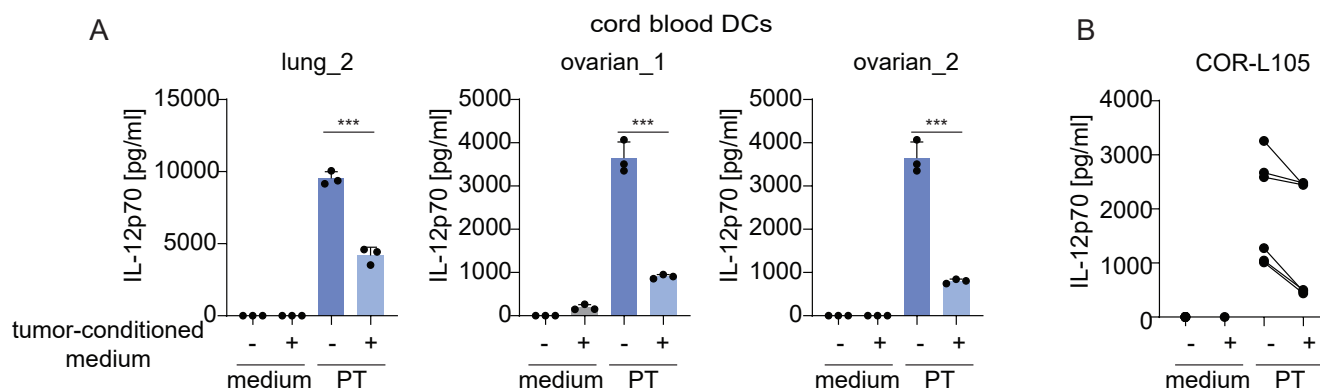
Supp. Figure 8 Poly(I:C) + TL8-506 activate cord blood cDCs to induce the release of IFN γ but not IL-4 or IL-10 in DC/T cell co-cultures. Sorted cord blood cDC2s were stimulated with the indicated stimuli for 18 hours. Treated cDCs were washed and co-cultured with allogeneic naive T cells for 4 days. Cytokine concentrations in the supernatant of co-cultures were determined by ELISA, n=2 batches of cord blood from mixed donors, 3 T cell donors, from two independent experiments, one-way ANOVA was used for statistical analysis, **p \leq 0.002. The following concentrations were used for DC stimulation: 10 μ g/mL Poly(I:C), 1 μ M TL8-506.

Figure S9



Supp. Figure 9 CCL4 and TNF α induce CD8⁺ T cell migration in 3D in vitro system. (A) Sorted cord blood cDC2s were stimulated for 18 hours with the indicated stimuli. Cytokine concentrations were determined in the cell culture supernatants by ELISA. CXCL10, CCL4 and TNF α concentrations in the supernatant of cDCs treated with IFN γ + TL8-506 or Poly(I:C) + TL8-506 are shown, n=3 batches of cord blood from mixed donors, 6 donors in total, from three independent experiments as described in Figure 1D. (B) Sorted cord blood cDC2s were stimulated with the indicated compounds for 18 hours. The supernatant was collected and placed into the bottom channel of a 3D tissue culture device. Activated CD8⁺ T cells were labeled with CMFDA and added to the top channel which was coated with an artificial endothelial vessel. T cell migration was measured after 48 hours by imaging of the collagen layer that separated the two channels. Cell counts of migrated CD8⁺ T cells in the absence (grey) and presence of 5 μ g/mL anti-CCL4 antibodies (green) in supernatants of stimulated cDCs are shown, n=2 donors, from two independent experiments, mean+SD, Student's t-test, ns, not significant. (C) Experimental set-up as described in B, CXCL10 + TNF α or CCL4 + TNF α dilutions in concentrations present in supernatants of IFN γ + TL8-506 or Poly(I:C) + TL8-506 treated cDC2s were placed in the bottom channel. Cell counts of migrated CD8⁺ T cells towards chemokine dilutions are depicted, n=2 donors, from two independent experiments, mean+SD, one-way ANOVA, **p \leq 0.002. The following concentrations were used for DC stimulation: 50'000 U/mL huIFN γ , 10 μ g/mL Poly(I:C), 1 μ M TL8-506.

Figure S10

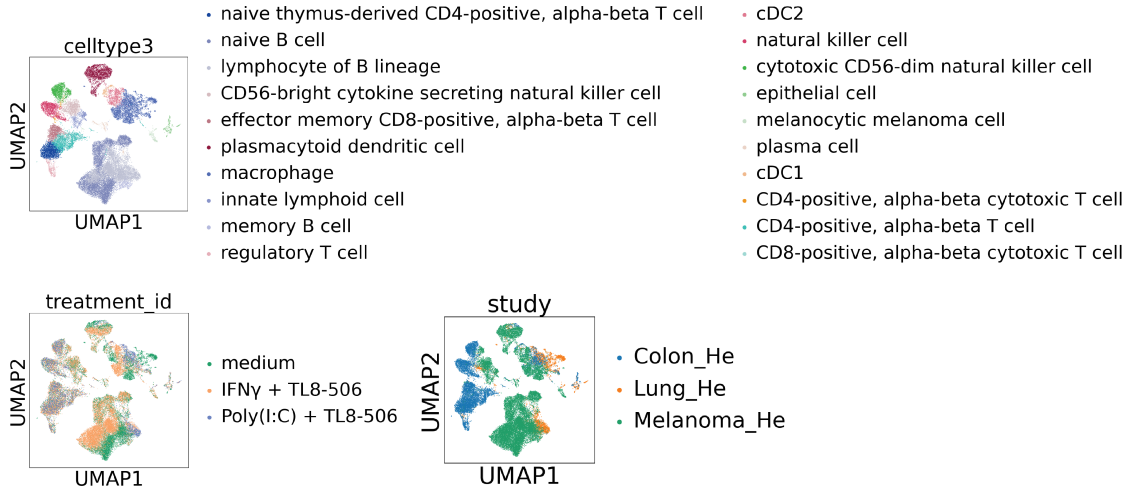


Supp. Figure 10 Poly(I:C) + TL8-506 activate cord blood cDCs in the presence of tumor-conditioned medium to produce IL-12p70. (A) Patient tumor-derived digest was cultured for 6 hours and tumor-conditioned medium was harvested. Sorted cord blood cDCs were stimulated with 1 μ M TL8-506 + 10 μ g/mL Poly(I:C) in the absence or presence of tumor-conditioned medium (1:1 diluted) for 16 hours. IL-12p70 concentrations were measured in cell culture supernatant by ELISA, 3 patient tumor-derived digests, 2 batches of cord blood from mixed donors (4 donors in total), from two independent experiments, mean+SD of technical replicates is shown, unpaired Student's t-test, *** $p \leq 0.0002$, PT = Poly(I:C) + TL8-506. (B) Cell culture supernatant of the human lung cancer cell line COR-L105 was collected. Sorted cord blood cDC2s were activated in the absence or presence of conditioned medium from COR-L105 cells for 16 hours. IL-12p70 concentrations were measured in cell culture supernatant by ELISA, 2 batches of cord blood from mixed donors (4 donors in total), from two independent experiments.

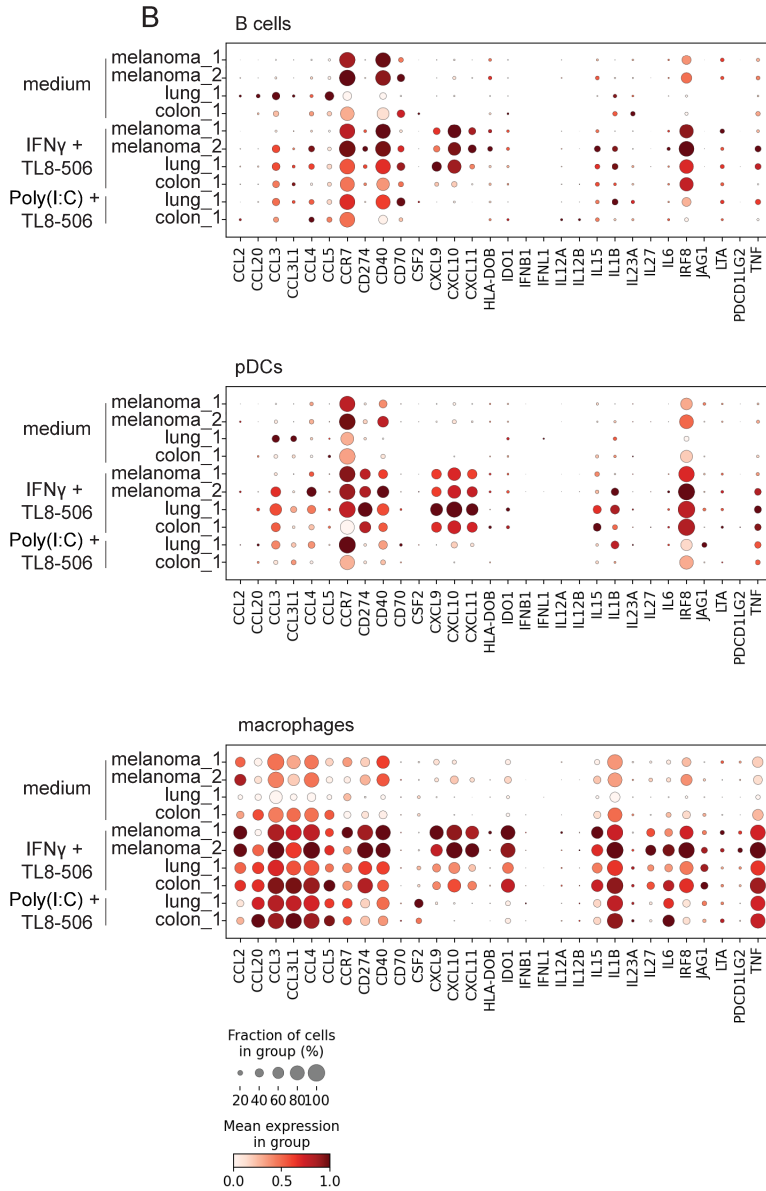
Figure S11

A

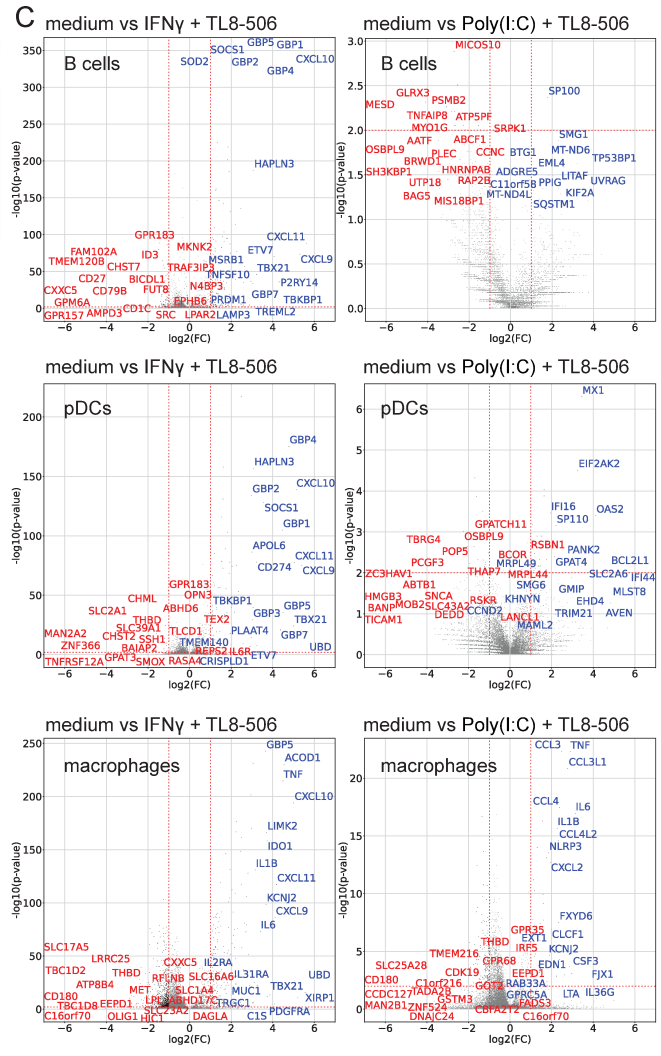
human tumor-derived immune cells



B

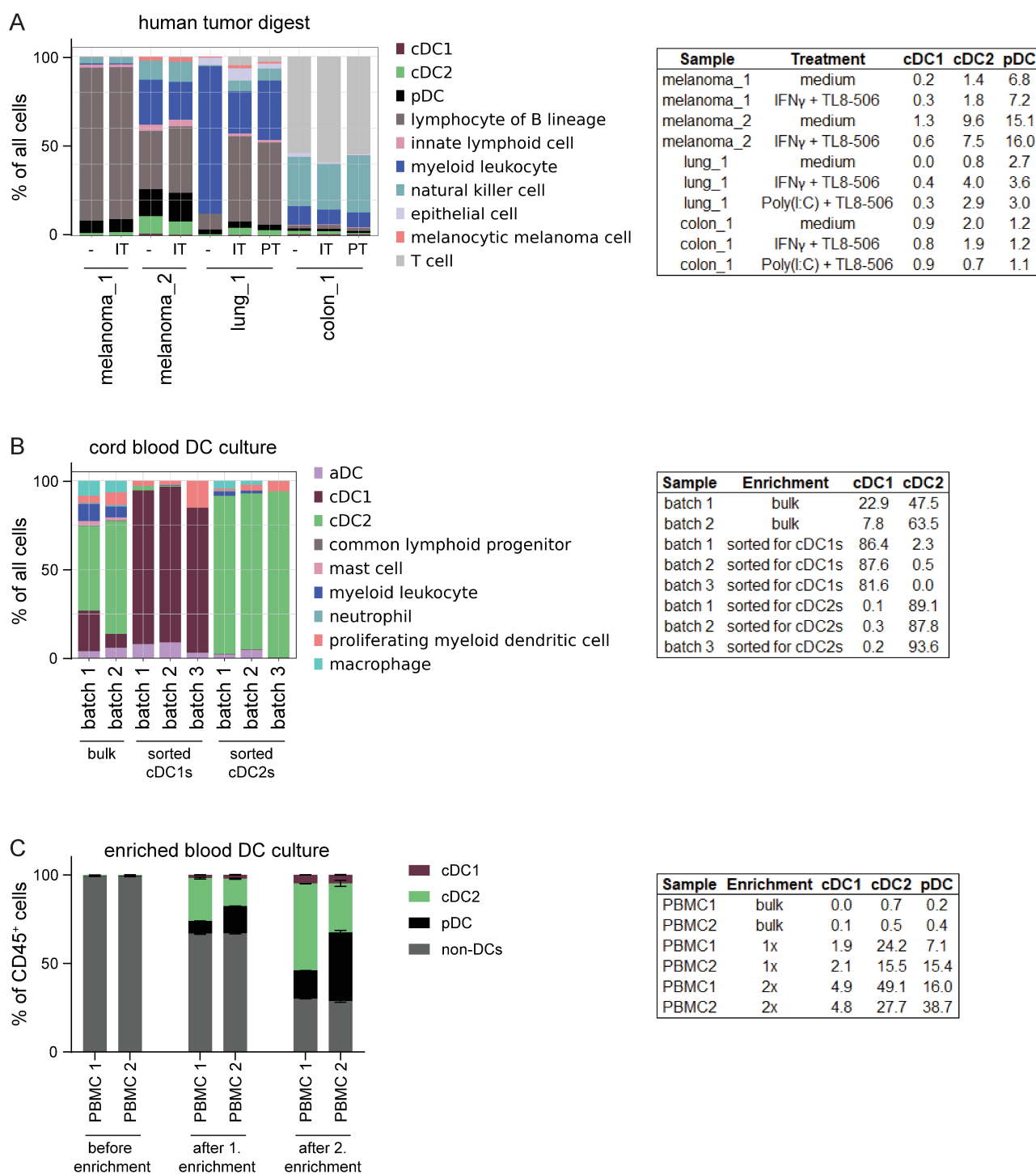


C



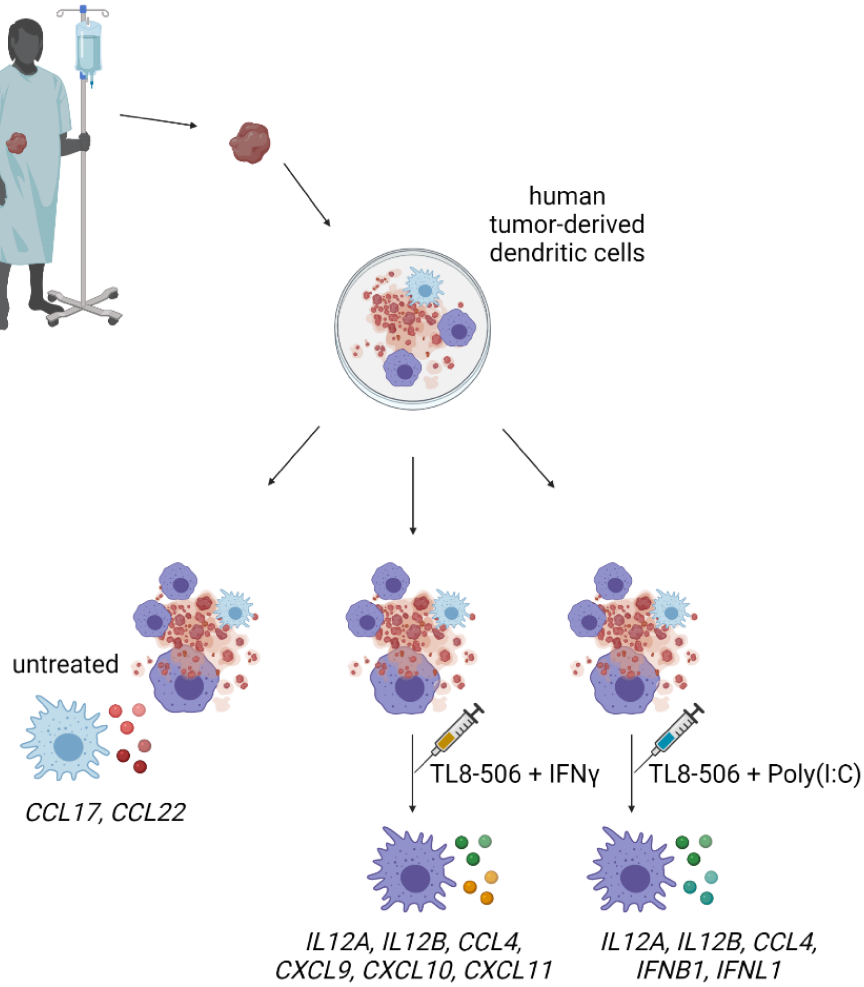
Supp. Figure 11 TL8-506 combinations up-regulate cytokines in human tumor-derived B cells, plasmacytoid DCs and macrophages in a cell type-specific manner. (A) UMAP of 35'169 cells profiled from IFN γ + TL8-506 or Poly(I:C) + TL8-506 treated and control treated tumor digests, with each cell color-coded for cell type, treatment and tissue. (B) Fraction positive and mean expression of activation markers in tumor-derived B cells, plasmacytoid DCs (pDCs) and macrophages upon treatment with TL8-506 combinations. Mean expression is calculated across all the cells in the group and then scaled to a 0-1 range. (C) Volcano plots showing differentially expressed (DE) genes (blue: up-regulated, red: down-regulated) between stimulated and control treated B cells, pDCs and macrophages from human tumor digests. Top 20 DE genes scored by p-values and fold changes are labeled, Wilcoxon Rank Sum test. The following concentrations were used for stimulation: 50'000 U/mL huIFN γ , 10 μ g/mL Poly(I:C), 1 μ M TL8-506.

Figure S12



Supp. Figure 12 Human cDCs are low in percentage in tumor tissue and blood. (A) Patient tumor-derived tissues were treated with the indicated compounds for 4 hours. 10x Genomics scRNA-seq was performed on FACS sorted CD45⁺, CD3⁻ cells with the exception of colon_1 that was sorted for CD45⁺ cells, n=4 donors, from three independent experiments. Percentages of DCs from all sequenced cells are plotted in a bar graph (left) or are listed in a table (right), - = medium, IT = IFN γ + TL8-506, PT = Poly(I:C) + TL8-506. (B) DCs were differentiated in vitro from cord blood stem cells, cells were harvested on day 12 and sorted for cDC1s, cDC2s or live cells (bulk) by FACS, 10x Genomics scRNA-seq was performed on sorted cells. n=3 batches of cord blood from mixed donors, 6 donors in total, from two independent experiments. Percentages of DCs from all sequenced cells are plotted in a bar graph (left) or are listed in a table (right). (C) PBMCs were isolated from buffy coats of healthy donors (bulk). DCs were enriched from PBMCs 1x or 2x using the Miltenyi Pan-DC Enrichment Kit, n=2 donors, from one experiment. Percentages of DCs from all CD45⁺ cells were quantified by flow cytometry and are plotted in a bar graph (left) or are listed in a table (right), mean+SD of technical replicates is shown.

Graphical Abstract



The graphical abstract was created with BioRender.com.

Combinations of Toll-like receptor 8 agonist TL8-506 activate human tumor-derived dendritic cells

Authors

Mi He, Bhavesh Soni, Petra C. Schwalie, Tamara Hüsser, Caroline Waltzinger, Duvini De Silva, Ylva Prinz, Laura Krümpelmann, Samuele Calabro, Ines Matos, Christine Trumpfheller, Marina Bacac, Pablo Umaña, Mitchell P. Levesque, Reinhard Dummer, Maries van den Broek, Stephan Gasser

Correspondence

mi.he@roche.com, stephan.gasser@roche.com

In Brief

- ☒ Human tumor-derived conventional dendritic cells (cDCs) from cancer patients are activated by Toll-like receptor 8 agonist combinations
- ☒ Human tumor-derived cDC1s and cDC2s show an immunostimulatory phenotype associated with Th1 responses upon treatment
- ☒ Combination-specific induction of activation markers are consistent in human cord blood, blood and tumor-derived cDCs